CHEMISTRY
AN ASIAN JOURNAL
ACES
FULL PAPER

DOI: 10.1002/asia.201300735

# Two-Photon Polarity Probes Built from Octupolar Fluorophores: Synthesis, Structure–Properties Relationships, and Use in Cellular Imaging

Céline Le Droumaguet,[c] Aude Sourdon,[b] Emilie Genin,[a] Olivier Mongin,*[b, c] and Mireille Blanchard-Desce*[a, c]

**Abstract:** A series of octupolar fluorophores built from a triphenylamine (TPA) core connected to electron-withdrawing (EW) peripheral groups through conjugated spacers has been synthesized. Their photoluminescence, solvatochromism, and two-photon absorption (2PA) properties were systematically investigated to derive structure–property relationships. All derivatives exhibit two 2PA bands in the 700–1000 nm region: a first band at low energy correlated with a core-to-periphery intramolecular charge transfer that leads to an intense 1PA in the blue-visible range, and a second more intense band at higher energy due to an efficient coupling of the branches through the TPA core. Increasing the strength of the EW end groups or the length of the conjugated spacers and replacing triple-bond linkers with double bonds induces both enhancement and broadening of the 2PA responses, thereby leading to cross-sections up to 2100 GM at peak and higher than 1000 GM over the whole 700–900 nm range. All derivatives exhibit intense photoluminescence (PL) in low- to medium-polarity environments (with quantum yields in the 0.5–0.9 range) and display a strong positive solvatochromic behavior (with Lippert–Mataga specific shifts ranging from 15000 to 27500 $cm^{-1}$), triple bonds, and phenyl moieties in the conjugated spacers, thereby leading to larger sensitivities than those of double bonds and thienyl moieties. More hydrophilic derivatives were also shown to be biocompatible, to retain their 2PA and PL properties in biological conditions, and finally to be suitable as polarity sensors for multiphoton cell imaging.

**Keywords:** absorption · bioimaging · chromophores · fluorescence · solvatochromism

## Introduction

Over the past decade, significant research efforts have been devoted to the molecular engineering of novel compounds that show very large two-photon absorption (2PA) responses.[1] These efforts were mostly driven by the advantages that 2PA provides (i.e., intrinsic 3D localization of excitation, excitation in the red-near-infrared (NIR) range to allow reduction of scattering losses) for applications in various domains that range from material science to biology and medicine. These include two-photon excited fluorescence (2PEF) microscopy for bioimaging,[2] localized photodynamic therapy (PDT),[3] localized release of bioactive species (of major interest in neurosciences),[4] 3D optical data storage,[5] optical power limiting,[6] and 3D microfabrication.[7] In this general framework, we have been interested more specifically in the design of innovative environmental two-photon fluorescent probes and sensors for biological applications and/or heavy-metal detection.[8] The ability of the probe to generate sufficient fluorescent signal is of major importance for detecting species of ultra-low concentration (such as heavy-metal traces or biomolecules in minute concentrations). This requires very large brightness to improve detection sensitivity (or alternatively the scanning speed in dynamic imaging of fast biological events). In this general framework, we have been interested in the design of sensitive two-photon fluorescent probes that combine very large 2PA responses in the NIR region as well as high sensitivity of their fluorescence to their microenvironment. With this aim in mind, we report the synthesis of a library of modular two-photon octupolar fluorophores with structural diversity (Figure 1), and the comprehensive study of structure–property (fluorescence–2PA–polarity sensitivity) relationships. By taking advantage of this investigation, we further designed more hydrophilic probes that were successfully applied to two-photon imaging in biological environments and micropolarity sensing in living cells.

[a] Dr. E. Genin, Dr. M. Blanchard-Desce
Université Bordeaux, Institut des Sciences Moléculaires
CNRS UMR 5255, 351 Cours de la Libération
33405 Talence Cedex (France)
Fax: (+33) 5-40-00-69-94
E-mail: m.blanchard-desce@ism.u-bordeaux1.fr

[b] A. Sourdon, Dr. O. Mongin
Institut des Sciences Chimiques de Rennes
CNRS UMR 6226, Université de Rennes 1
Campus de Beaulieu, 35042 Rennes Cedex (France)
Fax: (+33) 2-23-23-69-55
E-mail: olivier.mongin@univ-rennes1.fr

[c] Dr. C. Le Droumaguet, Dr. O. Mongin, Dr. M. Blanchard-Desce
Chimie et Photonique Moléculaires
CNRS UMR 6510, Université de Rennes 1
Campus de Beaulieu, F-35042 Rennes Cedex (France)

Supporting information for this article is available on the WWW under http://dx.doi.org/10.1002/asia.201300735.

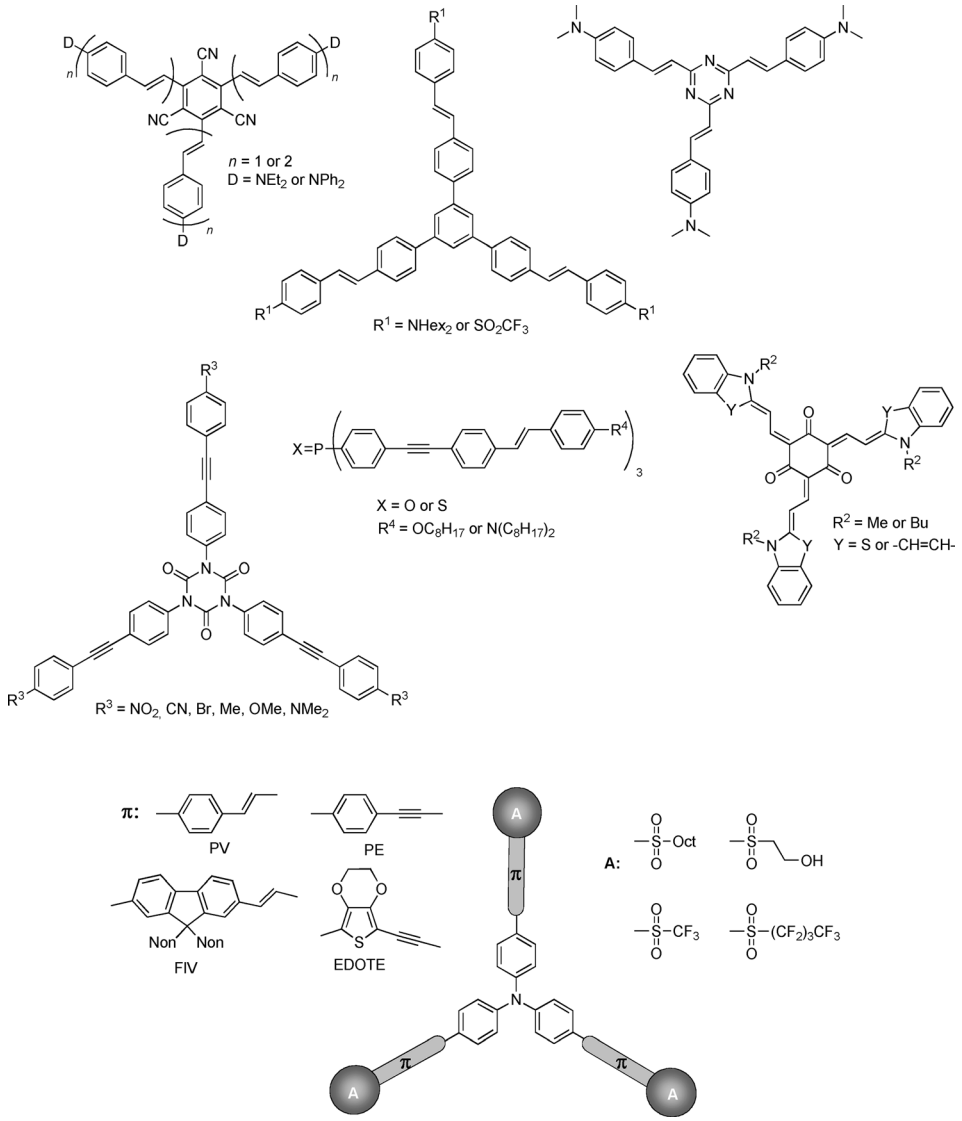


Figure 1. Selection of two-photon fluorescent three-branched octupolar compounds reported in the literature (derived from TCB,[11a] TPB,[14] triazine,[11b] triazinetrione (isocyanurate),[11c] TPPO,[13] TPPS,[13] cyclohexane-1,3,5-trione (phloroglucinol)[11d] cores), and the library reported in the present work.

## Results and Discussion

### Design

It has been now widely demonstrated that quadrupolar systems (centrosymmetrical conjugated molecules that bear two electron-releasing (D) or electron-withdrawing (A) end groups exhibit larger 2PA cross-section ($\sigma_2$) values than push–pull dipolar molecules (D group linked to A group with a conjugated moiety) in relation to a quadrupolar intramolecular charge transfer that takes place between the edges and the center of the molecules.[8a,9] Similarly, experimental and theoretical studies revealed that non-centrosymmetric octupolar systems typically built from the coupling of dipolar branches through specific common donor (D)[8d,10] or acceptor (A) cores[11] can lead to large 2PA responses. However, it has to be noted that the nature of the interactions between the dipolar branches in such branched systems (Figure 1) and consequently the photophysical and 2PA properties is strongly dependent on the nature of the common (D or A) core. Strongly nonadditive responses are observed in the case of the triphenylamine (TPA) donor moiety (which leads to the rise of a more intense 2PA band at higher energy, thereby corresponding to higher one-photon-forbidden, two-photon-allowed excited state, as expected from octupolar derivatives due to symmetry reasons)[12] or of the tricyanobenzene (TCB) acceptor moiety.[11a] In contrast, triphenylphosphane oxide (TPPO)- and triphenylphosphane sulfide (TPPS)-accepting cores[13] as well as the ambivalent triphenylbenzene (TPB)[14] core do not promote major 2PA enhancement linked to the rise of a new 2PA band at higher energy. Instead an almost additive behavior is observed and only broadening of the low-energy 2PA band (which corresponds to the low-energy, one-photon-allowed transition) is obtained, which can be possibly ascribed to through-space electrostatic interactions between branches. Hence the nature of the common D or A core is of major importance as long as giant 2PA responses are sought. Interestingly, in systems in which dipolar branches are assembled through a common D or A core, a localization of the excitation on one of the branches is observed prior to emission. As a result, their fluorescence is closely related to that of the dipolar chromophoric subunits, thus leading to a polar emissive excited state (and subsequent fluorescence solvatochromism).[12] On the basis of this analysis, we have shown earlier that elongated octupolar derivatives built from a TPA core and that bear potent electron-withdrawing (EW) peripheral moieties could lead to fluorescent probes that combine a large 2PA response and sensitivity to the polarity of their environment.[8d,10b] Herein, we present our continuing efforts in the comprehensive studies of structure–property relationships in a modular series of such derivatives (Figure 1) in which both the conjugated linkers and the

end groups are varied, focusing in particular on the combined effect of structural variation on 2PA and sensitivity to environment polarity. Rigid or semirigid conjugated spacers built from arylene–ethynylene and/or arylene–vinylene oligomers have been selected to allow efficient electronic communication between the TPA core and peripheral EW groups while preserving fluorescence.[9j] Selected arylenes are either aromatic (phenylene (P) and fluorenylene (Fl)) or heteroaromatic with reduced aromaticity (3,4-ethylenedioxythienylene (EDOT)) moieties. This latter heterocyclic moiety was chosen in light of shifting the emission to the red region, which is of interest for biological applications. In pursuit of our earlier efforts, we focused on peripheral moieties from the sulfone family, which show strong EW ability (with Hammett constants $\sigma_p$ larger than 0.8) and confer suitable and tunable solubility to the target octupolar derivatives relative to more classical cyano and nitro moieties. Electron-withdrawing (EW) groups that show increasing EW strength were used: from alkylsulfones ($SO_2Oct$, $\sigma_p \approx 0.8$) to triflyl moiety ($SO_2CF_3$, $\sigma_p \approx 1$) and perfluorobutylsulfone ($SO_2C_4F_9$, $\sigma_p \approx 1.1$).[10c,15] In addition, we prepared derivatives that bear $SO_2CH_2CH_2OH$ peripheral groups to induce a better solubility of the octupolar molecule in polar solvents or biological environments and provide the possibility for further functionalization and grafting onto biomolecules.

## Synthesis

We used a modular synthetic strategy to prepare the octupolar fluorophores that consist mainly of threefold coupling between a TPA core and functionalized building blocks. We focused on three different electron-releasing precursors, namely, triiodo-, trivinyl-, and triethynyl triphenylamine. Considering the need for carrying out three sequential repetitive reactions (due to the octupolar symmetry), we chose to focus on highly efficient methodologies. The elaboration of octupolar compounds with double-bond links was performed by means of Horner–Wadsworth–Emmons condensations or Heck couplings between vinyl and halogenated aromatic precursors. On the other hand, octupolar compounds that bear triple bonds were prepared by means of Sonogashira couplings between either the trihalogenated core and ethynyl arms or triethynyl core and halogenated derivatives. All new molecules have been fully characterized by NMR spectroscopy, HRMS, and elemental analysis data.

The extended iodinated building blocks **2a** and **2b** were obtained stereoselectively by condensations between *p*-iodobenzaldehyde and the corresponding phosphonates (**1a** and **1b**, respectively) in the presence of a base (sodium hydride and potassium *tert*-butoxide, respectively). The elongated arms **4a** and **4b** that contain a triflyl electron-withdrawing group were synthesized from bromo derivative **3b**: therefore, Heck coupling between **3b**[9j] and *p*-vinylbenzaldehyde[16] gave aldehyde **4a**, which was condensed with methyltriphenylphosphonium iodide to afford vinyl compound **4b** (Scheme 1). It should to be noted that these molecules

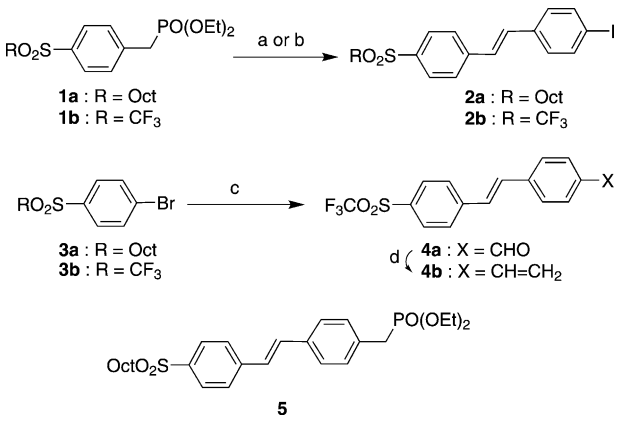


Scheme 1. Reagents and conditions: a) **1a**, 4-iodobenzaldehyde, NaH, THF, 20 °C, 15 h (61 % of **2a**); b) **1b**, 4-iodobenzaldehyde, *t*BuOK, $CH_2Cl_2$, 20 °C, 15 h (52 % of **2b**); c) **3b**, *p*-vinylbenzaldehyde, $K_2CO_3$, $Bu_4NCl$, $Pd(OAc)_2$, $PPh_3$, DMF, 110 °C, 10 h (26 %); and d) methyltriphenylphosphonium iodide (2.4 equiv), *t*BuOK, $CH_2Cl_2$, 20 °C, 4 h (51 %).

that bear very powerful electron-withdrawing groups (such as $SO_2CF_3$) are tricky substrates and represent a challenge in this kind of methodology in term of reactivity.

The synthesis of iodinated arm **7** that contained an EDOT moiety was achieved by Horner–Wadsworth–Emmons condensation between aldehyde **6**[17] and phosphonate **1b** in the presence of potassium *tert*-butoxide. Halogen–metal exchange on diiodofluorene **8a**,[9j] followed by quenching of the monolithio intermediate with DMF, afforded the nonsymmetrical fluorene **8b**, which was treated with phosphonate **1b** to lead to the iodine-bearing extended arm **9** as a mixture of *E*/*Z* stereoisomers (Scheme 2).

Perfluorobutylsulfone **11** building block was prepared according to a two-step alkylation/oxidation sequence in very good yields. Alkylation of *p*-bromothiophenol **10a** with 1-iodononafluorobutane led to **10b**, which was then oxidized with hydrogen peroxide in acetic acid to give sulfone **11**. Sulfone **13b**, which bears an alkyne group, was obtained from the corresponding bromo derivative **12**[18] with an excellent overall yield (91 %) by means of a palladium-catalyzed Sonogashira coupling with ethynyltrimethylsilane fol-

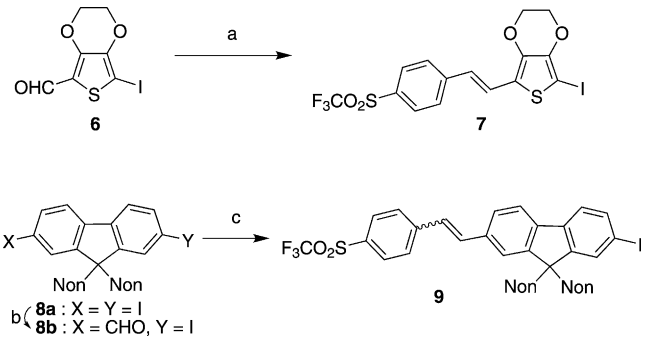


Scheme 2. Reagents and conditions: a) **1b** (1.1 equiv), *t*BuOK, $CH_2Cl_2$, 20 °C, 15 h (43 %); b) *n*BuLi, $Et_2O$, −78 °C to 20 °C, 30 min, then DMF, −78 °C to 20 °C, 15 h (27 %); and c) **1b** (1.1 equiv), *t*BuOK, $CH_2Cl_2$, 20 °C, 15 h (18 %). Non = *n*-nonyl.

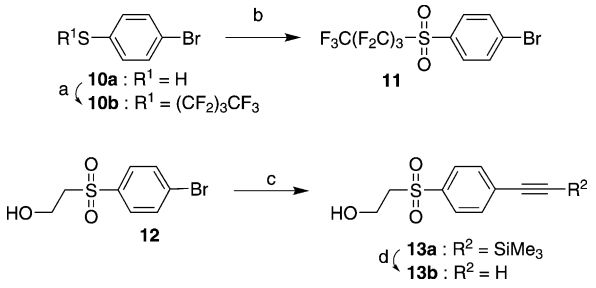


Scheme 3. Reagents and conditions: a) NaH, DMF, 20 °C, 1 h, then 1-iodo-nonafluorobutane, DMF, 20 °C, 2 h (92 %); b) $H_2O_2$, AcOH, reflux, 3 h (71 %); c) HC≡CSiMe$_3$, [Pd(PPh$_3$)$_2$Cl$_2$], CuI, Et$_3$N, toluene, 40 °C, 16 h (96 %); and d) NaOH, THF, 20 °C, 15 min (95 %).

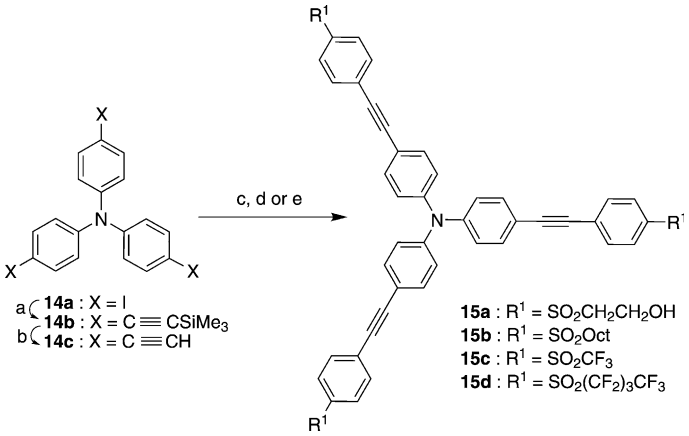


Scheme 4. Reagents and conditions: a) HC≡CSiMe$_3$, [Pd(Ph$_3$)$_2$Cl$_2$], CuI, NEt$_3$, toluene, 40 °C, 3 h (96 %); b) NaOH, THF, 20 °C, 35 h (87 %); c) **14a** (1 equiv), **13b** (4 equiv), [Pd(PPh$_3$)$_2$Cl$_2$], CuI, NEt$_3$, toluene, 40 °C, 15 h (78 % of **15a**); d) **14b** (1 equiv), **3a** or **3b** (3.5 equiv), [Pd$_2$(dba)$_3$] (dba = dibenzylideneacetone), CuI, PPh$_3$, tetra-*n*-butylammonium fluoride (TBAF), NEt$_3$, toluene, 35 °C, 22 h (65 % of **15b**, 84 % of **15c**); and e) **14c** (1 equiv), **11** (4 equiv), [Pd$_2$(dba)$_3$], CuI, PPh$_3$, NEt$_3$, toluene (47 % of **15d**).

lowed by a base-promoted deprotection of the trimethylsilyl group in the presence of sodium hydroxide (Scheme 3).

The same two-step alkylation/deprotection procedure was applied to convert the triiodo core **14a**[19] into the triethynylphenylamine derivatives **14b** and **14c** with excellent yields. The synthesis of the hydrophilic fluorophore **15a** was achieved with a good yield by means of a triple Sonogashira coupling of triiodo compound **14a** with alkyne **13b**. Core **14b** was used to prepare fluorophores **15b** and **15c** by treatment with bromo derivatives **3a** and **3b**, respectively, in a two-step, one-pot manner in the presence of fluoride ions, palladium(0), and copper iodide. This nice in situ deprotection/coupling procedure is a good way to avoid possible storage problems of the not-so-stable **14c** core. It is also a very efficient synthetic method as demonstrated by octupole **15c**, which was obtained by threefold Sonogashira reaction with 84 % yield, thereby resulting in an average yield of 94 % for each arm. Triple Sonogashira coupling of core **14c** with **11** also led efficiently to fluorophore **15d** with a yield of 78 % per branch (Scheme 4).

Extended octupoles **16a**, **16b**, and **17** were analogously synthesized with excellent yields by treating trialkynes **14b** or **14c** with extended iodo derivatives **2a**, **2b**, and **7**, respectively (Scheme 5). Vinylic fluorophores with alkylsulfonyl end groups **19a** and **19b** were obtained as pure all-*E* stereo-

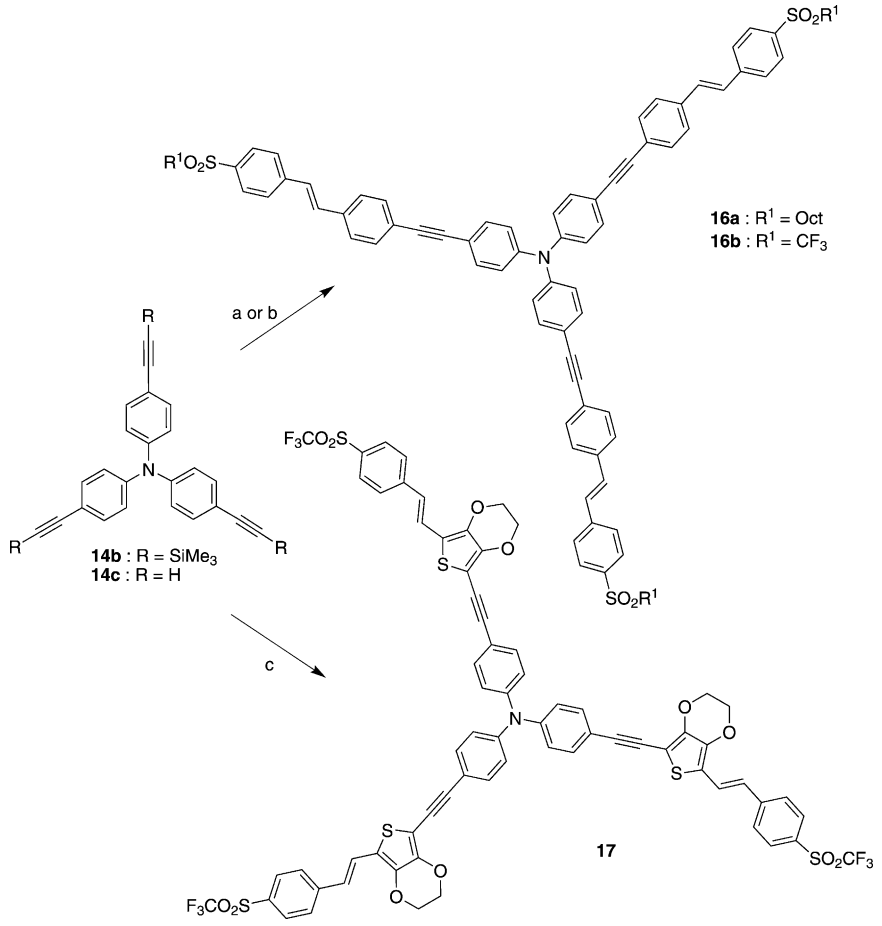


Scheme 5. Reagents and conditions: a) **14b** (1 equiv), **2a** (3.5 equiv), [Pd$_2$(dba)$_3$], CuI, PPh$_3$, TBAF, NEt$_3$, toluene, 20 °C, 65 h (89 % of **16a**); b) **14c** (1 equiv), **2b** (4 equiv), [Pd$_2$(dba)$_3$], CuI, PPh$_3$, NEt$_3$, toluene, 35 °C, 15 h (94 % of **16b**); and c) **14c** (1 equiv), **7** (3.5 equiv), conditions as in (b), 40 °C, 13 h (84 % of **17**).

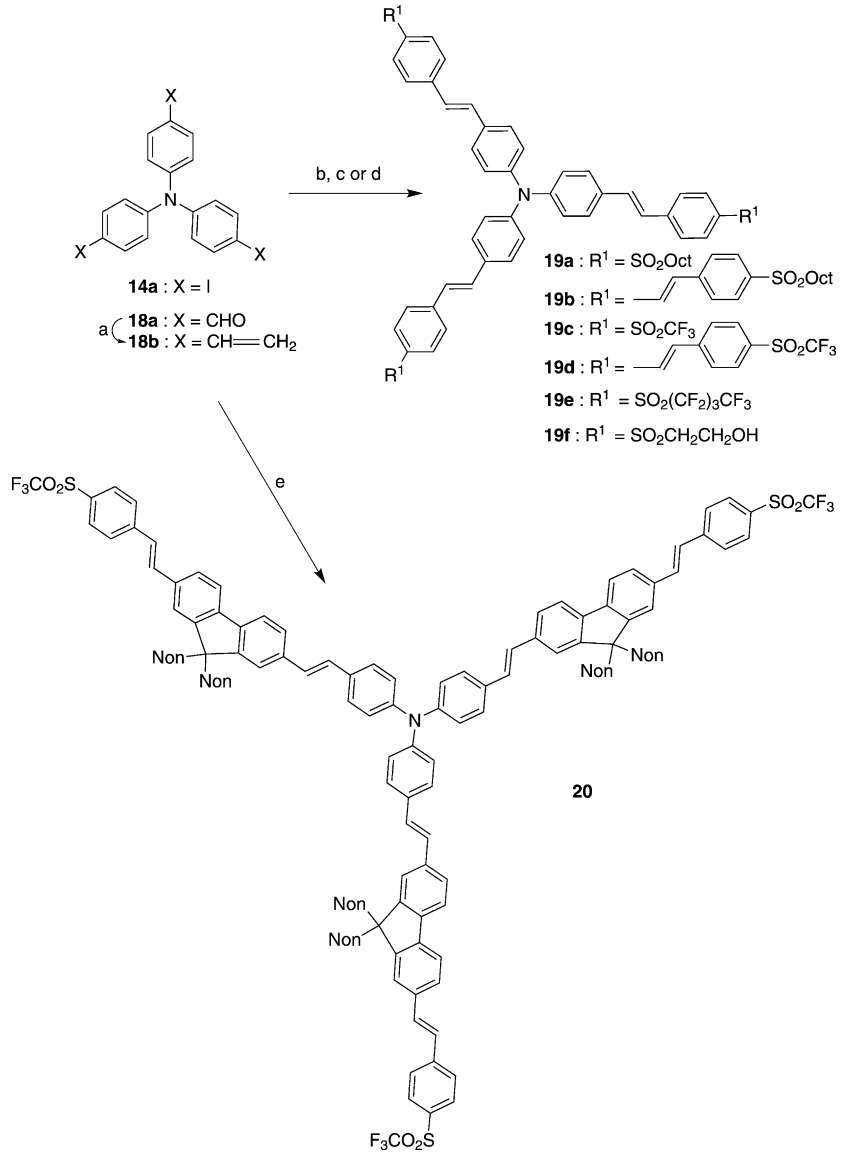


Scheme 6. Reagents and conditions: a) methyltriphenylphosphonium iodide, NaH, THF, RT, 15 h (99%); b) **18a** (1 equiv), **1a** or **5** (3.3 equiv), *t*BuOK, $CH_2Cl_2$, 20°C, 16 h, then reflux (36% of **19a**, 27% of **19b**); c) **18b** (1 equiv), **3b** or **11** or **12** (3.5–4 equiv), $Pd(OAc)_2$, $(o\text{-tol})_3P$, $NEt_3$, DMF, 100°C, 3 h (76% of **19c**, 55% of **19e**, 42% of **19f**); d) **14a** (1 equiv), **4b** (4.5 equiv), $Pd(OAc)_2$, $PPh_3$, $K_2CO_3$, $Bu_4NCl$, DMF, 90°C, 10 h (65% of **19d**); and e) **18b** (1 equiv), **9** (4 equiv), conditions as in (c), 110°C, 15 h (18% of **20**). Non = *n*-nonyl.

isomers, as testified by $^1H$ NMR spectroscopy, by a triple Horner–Wadsworth–Emmons condensation of trialdehyde core **18a**[20] with phosphonates **1a** and **5**, respectively, in the presence of potassium *tert*-butoxide but with quite low yields (Scheme 6). For the synthesis of the fluorophores with triflyl and perfluoroalkylsulfonyl end groups **19c**–**f** and **20**, an alternative pathway was thus considered, and they were prepared by means of triple Heck couplings starting from either triiodotriphenylamine **14a** or the trivinyl core **18b**, which resulted from the quantitative condensation between **18a** and methyltriphenylphosphonium iodide. Treatment of compound **18b** with brominated derivatives **3b**, **11**, and **12** afforded octupoles **19c**, **19e**, and **19f**, respectively, with quite good to very good yields and with all-*E* stereochemistry. In the same way, octupolar fluorophore **20**, which bears an extended fluorenylene–vinylene spacer, was synthesized by coupling between core **18b** and iodinated derivative **9**. Remarkably, it was also obtained with all-*E* stereochemistry, whereas starting material **9** was a mixture of *E*/*Z* stereoisomers. Two possible Heck couplings were tested for the preparation of fluorophore **19d** that bears two phenylene–vinylene moieties. The reaction between **18b** and **2b** with the catalytic system previously used was disappointing in this case. Alternatively, the assembly of triodo core **14a** and vinyl arm **4b** under Jeffery's conditions[21] afforded octupole **19d** with a 65% yield and with all-*E* stereochemistry as well (Scheme 6).

Finally, a dissymmetrical derivative **19g** that bears two triflyl end groups and a $SO_2CH_2CH_2OH$ extremity linked to phenylene–vinylene spacer was prepared by using the same type of Wittig condensation/Heck coupling two-step sequence (Scheme 7). The key step of this synthesis is the dissymmetrization of the triphenylamine core. This was achieved starting from trialdehyde **18a** by using only 1.5 equivalents of methyltriphenylphosphonium iodide, and derivative **18c** was obtained with an isolated yield of 31%. The desired octupole **19g** was then synthesized from the intermediate **18c** in three steps that involved double Heck coupling with bromo derivative **3b**, conversion of the remaining aldehyde into alkene, and final Heck coupling with bromo derivative **12**.

## Photophysical Properties

The photophysical data (absorption and fluorescence) of the synthesized octupolar derivatives built from a core TPA moiety are collected in Table 1 and include fluorescence quantum yields, lifetimes, and radiative and nonradiative decay rates values. All compounds display a broad absorp-

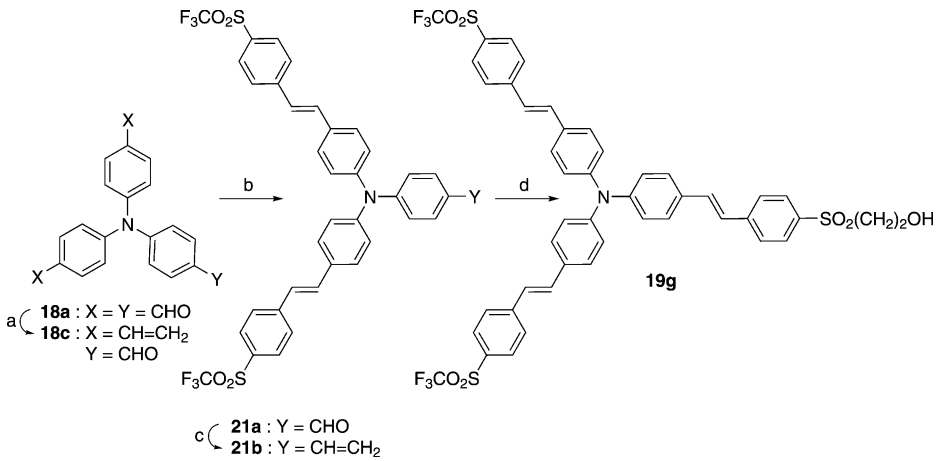


Scheme 7. Reagents and conditions: a) methyltriphenylphosphonium iodide (1.5 equiv), NaH, THF, RT (31%); b) **18c** (1 equiv), **3b** (3.5 equiv), $Pd(OAc)_2$, $(o\text{-tol})_3P$, $NEt_3$, DMF, 100°C (75%); c) methyltriphenylphosphonium iodide, NaH, THF, RT (54%); and d) **21b** (1 equiv), **12** (1.3 equiv), $Pd(OAc)_2$, $(o\text{-tol})_3P$, $NEt_3$, DMF, 100°C (53%).

All octupolar derivatives exhibit intense fluorescence emission in the visible region when dissolved in low-polarity solvents (such as toluene) or in ethanol (for compounds that bear $SO_2CH_2CH_2OH$ end groups) with fluorescence quantum yields that range from 0.52 to 0.93. Both the absorption and emission of these molecules can be tuned by modifying the strength of the peripheral electron-withdrawing end groups (Figure 2), the nature of the connector (or linker) between the TPA core and the end groups (Figures 3 and 4), or the length of the branches (Figure 3). Their fluorescence lifetimes (which range from 1 to 2 ns) and quantum yields (which range from 0.5 to 0.95) are also found to vary

tion in the near-UV blue-visible region associated with high molar extinction coefficients (up to $135000\,M^{-1}\,cm^{-1}$). A higher-energy, less-intense absorption band is observed in the UV region (300–350 nm).

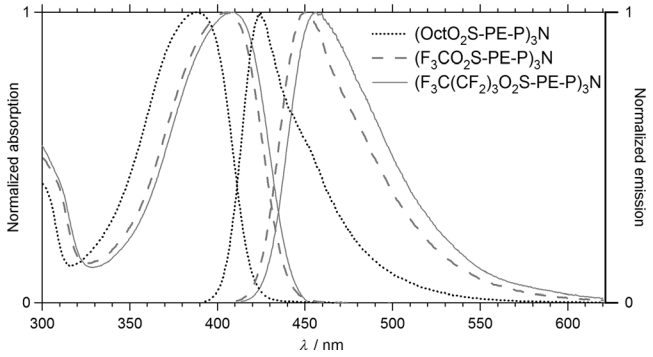


Figure 2. Absorption and emission spectra of **15b**, **15c**, and **15d** in toluene: EW effect of end groups.

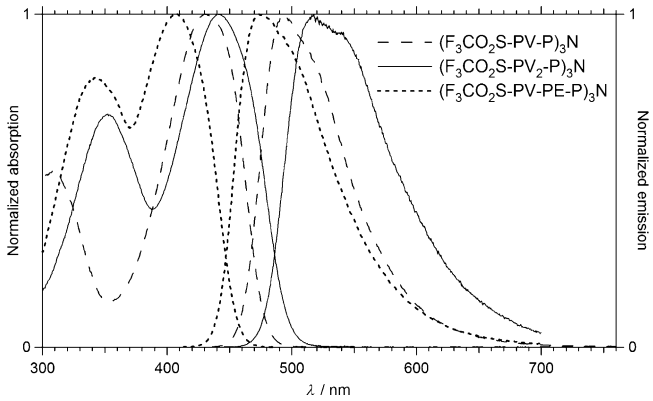


Figure 3. Absorption and emission spectra of **16b**, **19c**, and **19d** in toluene: Effects of conjugated linker and length.

Table 1. Photophysical properties of the series of octupolar chromophores and hydrophilic three-branched derivatives (in toluene).

| No. | Compound | End group (X=) | $\lambda_{max}^{abs}$ [nm] | $\log \varepsilon_{max}$ | $\lambda_{max}^{em}$ [nm] | Stokes shift [$cm^{-1}$] | $\Phi$[a] | $\tau$[b] [ns] | $k_r$[c] [$10^9\,s^{-1}$] | $k_{nr}$[d] [$10^9\,s^{-1}$] |
|---|---|---|---|---|---|---|---|---|---|---|
| **15b** | $(X\text{-PE-P})_3N$ | $SO_2Oct$ | 388 | 4.91 | 424 | 2100 | 0.77 | 1.27 | 0.62 | 0.18 |
| **15c** | $(X\text{-PE-P})_3N$ | $SO_2CF_3$ | 405 | 4.78 | 450 | 2470 | 0.78 | 1.49 | 0.52 | 0.15 |
| **15d** | $(X\text{-PE-P})_3N$ | $SO_2C_4F_9$ | 408 | 4.90 | 455 | 2510 | 0.90 | 1.51 | 0.60 | 0.07 |
| **16a** | $(X\text{-PV-PE-P})_3N$ | $SO_2Oct$ | 397 | 5.13 | 446 | 2770 | 0.79 | 1.35 | 0.59 | 0.20 |
| **16b** | $(X\text{-PV-PE-P})_3N$ | $SO_2CF_3$ | 408 | 4.97 | 474 | 3390 | 0.77 | 1.29 | 0.60 | 0.18 |
| **17** | $(X\text{-PV-EDOTE-P})_3N$ | $SO_2CF_3$ | 442 | 5.07 | 523 | 3500 | 0.52 | 1.00 | 0.52 | 0.48 |
| **19a** | $(X\text{-PV-P})_3N$ | $SO_2Oct$ | 410 | 4.90 | 463 | 2790 | 0.72 | 1.66 | 0.43 | 0.17 |
| **19c** | $(X\text{-PV-P})_3N$ | $SO_2CF_3$ | 430 | 4.91 | 494 | 2990 | 0.71 | 1.85 | 0.38 | 0.16 |
| **19e** | $(X\text{-PV-P})_3N$ | $SO_2C_4F_9$ | 435 | 4.90 | 499 | 2950 | 0.81 | 1.84 | 0.44 | 0.10 |
| **19b** | $(X\text{-PV}_2\text{-P})_3N$ | $SO_2Oct$ | 426 | 5.10 | 487 | 2940 | 0.77 | 1.23 | 0.63 | 0.19 |
| **19d** | $(X\text{-PV}_2\text{-P})_3N$ | $SO_2CF_3$ | 441 | 5.10 | 518 | 3380 | 0.84 | 1.51 | 0.56 | 0.11 |
| **20** | $(X\text{-PV-FlV-P})_3N$ | $SO_2CF_3$ | 435 | 5.07 | 498 | 2910 | 0.93 | 1.29 | 0.72 | 0.05 |
| **15a** | $(X\text{-PE-P})_3N$ | $SO_2CH_2CH_2OH$ | 389 | – | 430 | 2450 | 0.70 | 1.25 | 0.56 | 0.24 |
| **19f** | $(X\text{-PV-P})_3N$ | $SO_2CH_2CH_2OH$ | 415 | – | 469 | 2750 | 0.70 | 1.94 | 0.36 | 0.15 |
| **19g** | $(X_1\text{-PV-P})_2(X_2\text{-PV-P})N$ | $SO_2CF_3/SO_2CH_2CH_2OH$ | 425 | 4.83 | 498 | 3500 | 0.77 | 1.75 | 0.44 | 0.13 |

[a] Fluorescence quantum yield determined relative to fluorescein in 0.1 M NaOH.[22] [b] Fluorescence lifetime determined using time-correlated single-photon counting (TCSPC). [c] Radiative decay rate, $k_r = \Phi/\tau$. [d] Nonradiative decay rate, $k_{nr} = (1-\Phi)/\tau$.

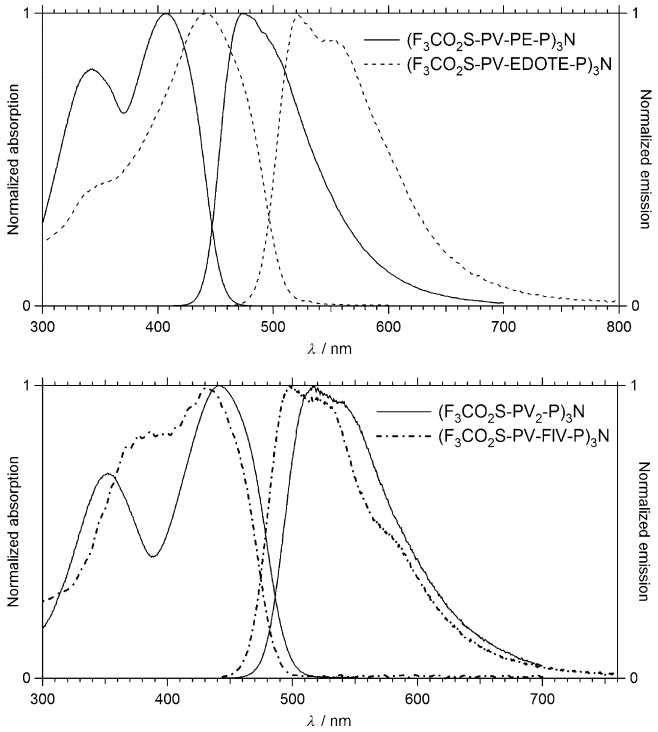


Figure 4. Absorption and emission spectra of **16b** and **17** (top); **19d** and **20** (bottom) in toluene: effect of arylene connector.

to some extent depending on the octupolar structures (Table 1).

*Effect of End Groups*

Comparisons of the series of octupolar derivatives with a phenylene–ethylene spacer (**15b**, **15c**, **15d**) or with a phenylene–vinylene one (**19a**, **19c**, and **19e**) show that increasing the electron-withdrawing strength of the end groups induces a bathochromic shift of both the absorption and emission bands (Figure 2 and Table 1). The magnitude of the bathochromic effect is correlated to the EW strength of the end groups, as expected from a periphery-to-core intramolecular charge-transfer (ptc-ICT) phenomenon.[10c] The Stokes shifts values are also found to increase along with the EW strength, which is indicative of a larger nuclear reorganization in the excited state and is in agreement with more pronounced ptc-ICT (or more precisely larger excited-state dipole moments; see below). We note, however, that the increase in EW strength does not induce an increase in one-photon absorptivity (Table 1), which is in contrast to what is obtained when tuning the length and nature of the connecting branches (see below).

Interestingly, fluorescence quantum yield values remain high even though their emission is redshifted. This phenomenon is a consequence of the singular decrease in the nonradiative decay rates (Table 1), most probably in relation to the fluorinated nature of the perfluoroakyl sulfone moieties ($SO_2CF_3$ and $SO_2C_4F_9$), which are responsible for a reduction in the vibrational deactivation processes. As a result, these derivatives also show slightly longer fluorescence lifetimes than their alkylsulfone ($SO_2Oct$) analogues owing to combined reduction of radiative and nonradiative decay rates (Table 1).

*Effect of the Nature of the Conjugated Linker*

As expected and already observed in the case of quadrupolar derivatives,[9j] replacing a triple bond by a double bond in the conjugated connector induces a bathochromic shift in both absorption and emission (Figure 3 and Table 1). Once again the emission band redshifts are usually larger, thus leading to larger Stokes shift values, which is indicative of larger nuclear reorganization in the excited state after excitation prior to emission. In contrast, the replacement of a triple bond with a double bond in the conjugated linkers does not significantly affect the one-photon absorptivity (thus leading to almost unchanged extinction coefficients), nor does it affect the fluorescence quantum yields, which are maintained. This results from the combined reduction of radiative (as expected from redshifted emission)[23] and nonradiative decay rates. It is important to note that the triple bond—although it confers improved rigidity (reducing conformational flexibility)—does not result in lower nonradiative rates (as commonly expected from the rigidity/fluorescence paradigm). Such an effect is not uncommon[9j] and provides evidence of active vibrational modes. The fluorescence lifetimes are somewhat longer for derivatives with double bonds instead of triple bonds in the conjugated linker, thanks to a slower radiative decay in relation to the redshifted emission. Interestingly, elongated octupolar fluorophores that bear a triflyl moiety, **16b** and **19d**, display a singular behavior; the replacement of the triple bond with a double bond in the conjugated linker leads to an increase in the quantum yield value in relation to a marked decrease in nonradiative decay and lack of decrease in the radiative decay. In that particular case, the effect of redshifted emission is compensated by a hyperchromic effect, thereby resulting in the conservation of the radiative rate.[23]

In contrast, changing the nature of the arylene connector in conjugated linkers can significantly affect not only the position of the absorption and emission bands but also the fluorescence quantum yield and lifetime values. As illustrated in Figure 4, the replacement of a phenyl unit with an EDOT moiety induces a marked bathochromic shift in both absorption and emission bands as well as a hyperchromic effect and reduction in both fluorescence quantum yield and lifetime values (Table 1). The EDOT unit leads to a larger nonradiative decay rate (probably in connection with favored intersystem crossing), whereas the radiative decay rate is maintained.

On the contrary, both the absorption and emission bands are slightly blueshifted when the phenyl unit is replaced with a fluorenylene moiety (Figure 4), which also induces a marked hypochromic effect. Interestingly, the nonradiative decay is significantly slowed (most probably in relation with decreased vibrational deactivation), whereas the radiative decay rate significantly increases (Table 1). As a result, the octupolar fluorophore built from the fluorenylene–vinylene

conjugated linkers **20** displays the largest fluorescence quantum yield in the series. These observations confirm that fine tuning of the fluorescence properties can be achieved through systematic structural variations, which are made possible on account of the modular approach implemented.

*Effect of the Length of the Conjugated Linker*

Increasing the length of the conjugated linker between the TPA core and the EW peripheral groups by adding a phenylene–vinylene (PV) unit induces a bathochromic (and hyperchromic effect) shift in both the absorption and emission bands, as well as a marked spectral broadening of the absorption and increase in the Stokes shift values (Figure 3). This is consistent with efficient ptc-ICT, thus indicating that the linkers are indeed acting as efficient conjugating connecting modules. Although a lengthening of the conjugated linker does not influence the nonradiative decay, the radiative decay undergoes a definite enhancement, most probably in relation to the marked hyperchromic effect that parallels an increase in the transition dipole between the emitting excited state and the ground state. This leads to a slight increase in the fluorescence quantum yields and to significantly shorter fluorescence lifetimes (Table 1).

When increasing the length of the conjugated linker between the TPA core and the EW peripheral groups by adding a phenylene–ethynylene (PE) unit instead, a marked hyperchromic shift and spectral broadening is also observed. However, a hypsochromic shift in both the absorption and emission bands is observed (Figure 3) in contrast to the effect of phenylene–vinylene unit insertion. As a result, the radiative decay rates significantly increase, thereby leading—also in that case—to the enhancement of fluorescence quantum yield (but shorter lifetimes than the elongated compound with a PV2 linker; Table 1). Hence, increasing the linker length by inserting PE or PV units indeed allows one to increase the brightness ($\varepsilon_{max}\Phi$) of the octupolar fluorescent probes reported in this work. This validates the molecular engineering strategy implemented here for octupolar derivatives derived from a TPA core, as also observed for rodlike quadrupolar derivatives built from ambivalent (i.e., weak donor/acceptor) biphenyl, fluorenyl,[9e,j] and dihydrophenanthrene[8a] cores but with similar connecting units between the core and terminal electroactive end groups. Interestingly, inserting a fluorenylene–vinylene (Fl–V) unit into the conjugated linker allows one to bathochromically (and hyperchromically) shift both the absorption and emission while increasing the fluorescence quantum yield (Table 1, comparison of compounds **19c** and **20**). This confirms that changing the nature of the arylene connecting unit in the conjugated linker can be used to both tune the position and the intensity of the emission band.

*Polarity Sensing*

Solvent effects on the photophysical properties of the library of octupoles were then investigated to gain better insight into the nature of the emissive excited state and derive structure–sensitivity relationships, thereby allowing one to optimize the potential of the investigated octupolar derivatives as (micro)polarity probes. As illustrated in Figure 5 for molecules **16b** and **17**, all octupolar derivatives behave nicely as fluorescent polarity probes: increasing the solvent

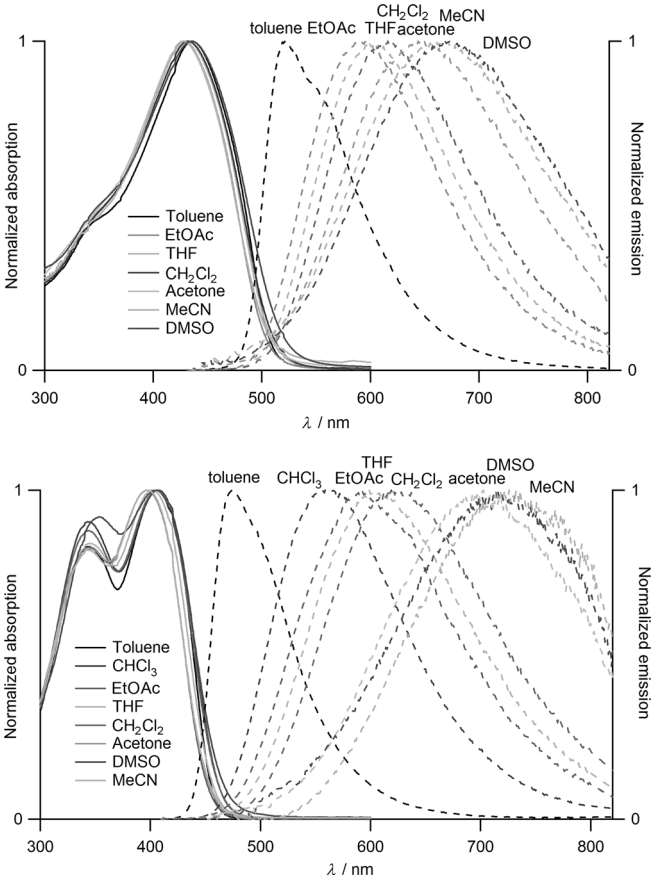


Figure 5. Solvatochromic behavior of octupolar fluorophores **17** (top) and **16b** (bottom).

polarity induces only a slight bathochromic shift in the absorption band but produces a marked redshift (and broadening) in the fluorescence emission band. Accordingly, the Stokes shift values significantly increase along with an increase in solvent polarity. Such positive solvatochromic behavior is consistent with a ptc-ICT phenomenon, thereby leading after excitation, and prior to emission, to the localization of the excitation on the dipolar chromophoric branches.[12] As a result, highly polar emissive excited states are obtained, which are stabilized by polar solvents to result in redshifted emission. Indeed, the Stokes shift values were found to depend linearly on the polarity–polarizability parameter $\Delta f$ (Figure 6) in agreement with the Lippert–Mataga relationship [Eq. (1)].[24]

$$\nu_{abs} - \nu_{em} = 2\Delta\mu^2\Delta f/(hca^3) + \text{const} \quad (1)$$

for which $\nu_{abs}$ ($\nu_{em}$) is the wavenumber of the absorption (fluorescence) maximum, $\Delta\mu$ is the change in the dipole moment between the relaxed emissive excited state and cor-

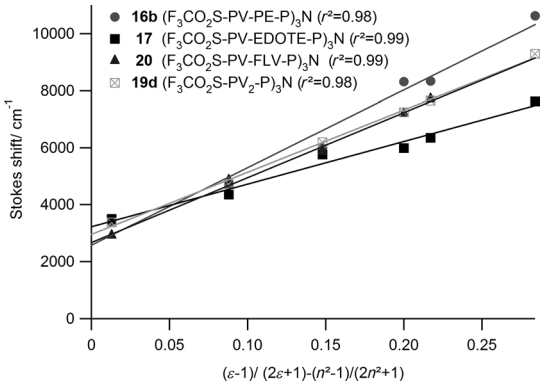


Figure 6. Lippert–Mataga correlations for octupolar compounds **16b**, **19d**, **17**, and **20**.

responding Frank–Condon ground state, $h$ is the Planck constant, $c$ is the light velocity, $a$ is the radius of the Onsager spherical cavity, and $\Delta f=(\varepsilon-1)/(2\varepsilon+1)-(n^2-1)/(2n^2+1)$, in which $\varepsilon$ is the dielectric constant and $n$ the refractive index of the solvent.

The slope values derived from the Lippert–Mataga linear correlations for all octupolar chromophores are collected in Table 2. These specific shift values allow one to quantify the sensitivity to solvent polarity and rank the different synthetic derivatives as fluorescent (micro)polarity probes.[25] We observed that the specific shift values determined for all octupolar derivatives are quite high (they vary from 15 to $27\times10^3$ cm$^{-1}$); the largest ones approach that of the best fluorescent polarity probes despite their significant size.[26] This confirms the interest in such derivatives for polarity sensing. In that respect, molecular optimization can be achieved as the sensitivity to solvent polarity is found to be strongly dependent on structural/electronic features. Indeed, both the strength of the peripheral EW end groups and the length and nature of the conjugated linkers are found to influence the sensitivity of the fluorescent probes (Table 2). More precisely, we observe that increasing the electron-withdrawing strength of the end groups induces a pronounced amplification of the fluorescence sensitivity on the solvent polarity as illustrated by the comparison of compounds **15b–d** or **16a–b**. We also observe that in most cases, compounds that bear a more rigid spacer (i.e., with a triple bond instead of a double bond) display larger specific shift values when comparing related octupoles that contain either short (**15c**, **15d** and **19c**, **19e**, respectively) or extended conjugated paths (**16b** and **19d** in Figure 6). Interestingly, a further increase in the specific shift values can be achieved by adding a phenylene–vinylene unit and consequently lengthening the conjugated spacer as shown by a comparison of compounds **19a** and **19b** that bear $SO_2$Oct end groups. This phenomenon is even more pronounced with octupoles **19c** and **19d**, which contain stronger electron-withdrawing terminal moieties (Table 2).

Finally, the nature of the π connector in the dipolar branches is found to significantly influence the polarity sensitivity of the octupolar probes. Indeed, replacing a phenyl unit with a less aromatic EDOT moiety leads to a pronounced decrease in solvatochromic behavior, as indicated by comparison of **16b** and **17** (Figure 5), whereas the replacement with a fluorenyl connector induces a slight increase of the solvatochromic behavior, as indicated by comparison of **19d** and **20** (Figure 6).

From the specific shift values derived from the Lippert–Mataga relationship, which are directly related to $\Delta\mu/a^3$ [Eq. (1)], we could derive $\Delta\mu$ values by using estimated $a$ values calculated by considering the dipolar branches as emissive dipoles (Table 2).[27] We observe that the octupolar derivatives that combine the stronger EW peripheral groups ($SO_2CF_3$) as well as the longer branches and more rigid connectors led to the largest $\Delta\mu$ values (up to 42 D), thereby providing evidence of highly polarized emissive excited

Table 2. Solvatochromic data of the series of octupolar chromophores and hydrophilic three-branched derivatives.

| No. | Compound | End group (X=) | Specific solvatochromic shift[a] [$10^3$ cm$^{-1}$] | $l$[b] [Å] | $a$[c] [Å] | $\Delta\mu$[d] [D] |
|---|---|---|---|---|---|---|
| **15b** | (X-PE-P)$_3$N | $SO_2$Oct | 14.6 | 12.9 | 5.2 | 14.2 |
| **15c** | (X-PE-P)$_3$N | $SO_2CF_3$ | 19.7 | 12.9 | 5.2 | 16.5 |
| **15d** | (X-PE-P)$_3$N | $SO_2C_4F_9$ | 23.4 | 12.9 | 5.2 | 17.9 |
| **16a** | (X-PV-PE-P)$_3$N | $SO_2$Oct | 24.4 | 19.4 | 7.7 | 33.5 |
| **16b** | (X-PV-PE-P)$_3$N | $SO_2CF_3$ | 27.2 | 19.4 | 7.7 | 35.4 |
| **17** | (X-PV-EDOTE-P)$_3$N | $SO_2CF_3$ | 15.6 | 18.9 | 7.5 | 25.8 |
| **19a** | (X-PV-P)$_3$N | $SO_2$Oct | 15.5 | 12.5 | 5.0 | 13.9 |
| **19c** | (X-PV-P)$_3$N | $SO_2CF_3$ | 15.2 | 12.5 | 5.0 | 13.8 |
| **19e** | (X-PV-P)$_3$N | $SO_2C_4F_9$ | 16.8 | 12.5 | 5.0 | 14.5 |
| **19b** | (X-PV$_2$-P)$_3$N | $SO_2$Oct | 17.9 | 17.6 | 7.0 | 24.8 |
| **19d** | (X-PV$_2$-P)$_3$N | $SO_2CF_3$ | 21.8 | 17.6 | 7.0 | 27.4 |
| **20** | (X-PV-FlV-P)$_3$N | $SO_2CF_3$ | 23.5 | 23.0 | 9.2 | 42.6 |
| **15a** | (X-PE-P)$_3$N | $SO_2CH_2CH_2OH$ | 17.0 | 12.9 | 5.2 | 15.3 |
| **19f** | (X-PV-P)$_3$N | $SO_2CH_2CH_2OH$ | 18.9 | 12.5 | 5.0 | 15.4 |
| **19g** | (X$_1$-PV-P)$_2$(X$_2$-PV-P)N | $SO_2CF_3$/$SO_2CH_2CH_2OH$ | 20.0 | 12.5 | 5.0 | 15.8 |

[a] Absolute value of the slope derived from the linear dependence of the Stokes shift on the polarity/polarizability function of the solvent ($\Delta f=(\varepsilon-1)/(2\varepsilon+1)-(n^2-1)/(2n^2+1)$, in which $\varepsilon$ is the dielectric constant and $n$ the refractive index). [b] Distance from the core N atom to the peripheral S atom. [c] Onsager cavity radius (estimated from $a=0.4l$). [d] Change of dipole between the relaxed emissive excited state and corresponding Frank–Condon ground state.

states as the origin of the large sensitivity toward environment polarity.

### Two-Photon Absorption

Thanks to their strong fluorescence, the 2PA response of all derivatives in the NIR region could be experimentally determined by using the well-known two-photon-induced fluorescence (2PEF) technique following the methodology developed and fully documented by Webb and collaborators.[9b,28] As illustrated in Figures 7 and 8, all molecules display broad

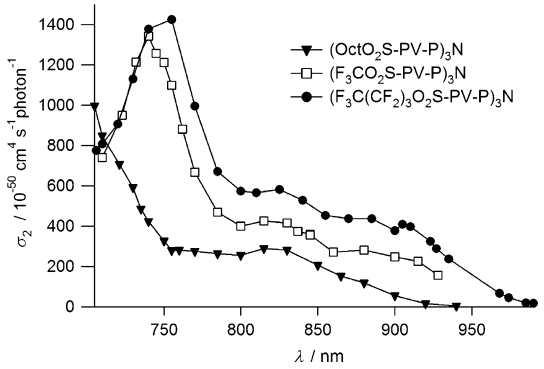


Figure 7. Two-photon absorption spectra of compounds **19a**, **19b**, and **19e**: effect of the (EW) strength of the peripheral groups.

and intense 2PA bands in the 700–1000 nm region. We observe that the first 2PA maxima occurs at about twice the wavelength of the low-energy intense one-photon absorption band, which indicates that the lowest excited state is both one- and two-photon allowed (as reported earlier for octupolar derivatives built from TPA core[12,27] as well for different three-branched derivatives[13,14]). In addition, much more intense and broad 2PA bands are observed at higher energy,

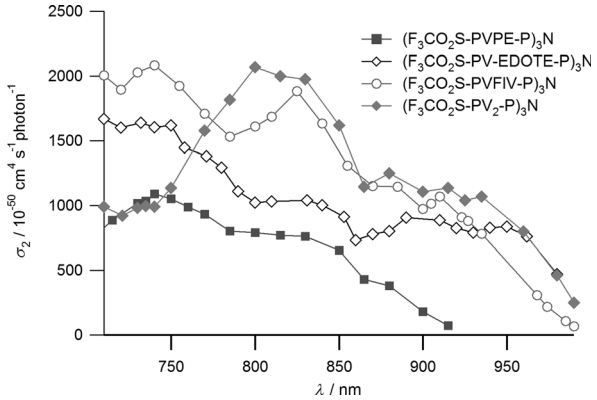


Figure 8. Two-photon absorption spectra of compounds **16b**, **17**, **20**, and **19d**: effect of conjugated spacer.

which is promoted by the efficient electronic coupling between the branches provided by the TPA core.[12,27]

*Effect of End Groups*

A comparison of octupoles that bear different EW groups shows that increasing the acceptor strength leads to both an enlargement of the 2PA band in the near-IR region and a significant enhancement of the $\sigma_2$ values, typically by a factor of 1.5 to 2.5 for the peak 2PA cross-sections, as illustrated in Figure 7 and observed from Table 3. The introduction of the OH functions as appending moieties provides solubility in hydrophilic and alcoholic environments, which in turn leads to a sizeable increase in the 2PA responses (**15b** and **19a** compared to **15a** and **19f**, respectively).

*Effect of the Conjugated Linker*

The comparison of compounds **16b** and **19d** shows that replacing a phenylene–ethynylene unit with a phenylene–vinylene unit results classically in a large redshift of the 2PA spectrum and a pronounced enhancement of the 2PA peak cross-sections (Figure 8). Nevertheless, octupolar fluoro-

Table 3. Two-photon absorption properties of the series of octupolar chromophores and three-branched hydrophilic derivatives (in toluene).

| No. | Compound | End group (X=) | $2\lambda_{max}^{abs}$ [nm] | $\lambda_{max1}^{2PA}$ [nm] | $\sigma_2$ at $\lambda_{max1}^{2PA}$ [GM][a] | $\lambda_{max2}^{2PA}$ [nm] | $\sigma_2$ at $\lambda_{max2}^{2PA}$ [GM][a] |
|---|---|---|---|---|---|---|---|
| **15b** | (X-PE-P)$_3$N | $SO_2Oct$ | 776 | 750 | 180 | – | – |
| **15c** | (X-PE-P)$_3$N | $SO_2CF_3$ | 810 | 800 | 370 | $\leq$705 | $\geq$700 |
| **15d** | (X-PE-P)$_3$N | $SO_2C_4F_9$ | 816 | 825 | 400 | $\leq$705 | $\geq$995 |
| **16a** | (X-PV-PE-P)$_3$N | $SO_2Oct$ | 794 | 815 | 590 | 715 | 1085 |
| **16b** | (X-PV-PE-P)$_3$N | $SO_2CF_3$ | 816 | 800 | 790 | 740 | 1090 |
| **17** | (X-PV-EDOTE-P)$_3$N | $SO_2CF_3$ | 884 | 890 | 790 | $\leq$710 | $\geq$1670 |
| **19a** | (X-PV-P)$_3$N | $SO_2Oct$ | 820 | 815 | 290 | $\leq$705 | $\geq$995 |
| **19c** | (X-PV-P)$_3$N | $SO_2CF_3$ | 860 | 880 | 280 | 740 | 1340 |
| **19e** | (X-PV-P)$_3$N | $SO_2C_4F_9$ | 870 | 885 | 440 | 755 | 1425 |
| **19b** | (X-PV$_2$-P)$_3$N | $SO_2Oct$ | 852 | 880 | 475 | 770 | 1510 |
| **19d** | (X-PV$_2$-P)$_3$N | $SO_2CF_3$ | 882 | 880 | 1250 | 800 | 2070 |
| **20** | (X-PV-FlV-P)$_3$N | $SO_2CF_3$ | 870 | 885 | 1145 | 740 | 2080 |
| **15a**[b] | (X-PE-P)$_3$N | $SO_2CH_2CH_2OH$ | 768 | 750 | 270 | $\leq$700 | $\geq$300 |
| **19f**[b] | (X-PV-P)$_3$N | $SO_2CH_2CH_2OH$ | 822 | 820 | 360 | 715 | 800 |
| **19g**[b] | (X$_1$-PV-P)$_2$(X$_2$-PV-P)N | $SO_2CF_3$/$SO_2CH_2CH_2OH$ | 850 | 820 | 490 | 740 | 950 |

[a] 1 GM = $10^{-50}$ cm$^4$s$^{-1}$photon$^{-1}$. [b] In ethanol.

phores that contain triple bonds have the advantage to be more photostable and rigid than their analogues with double bonds. We observe from Figure 8 that increasing the length of the arms induces a further marked enhancement of the 2PA properties, which follows the trend observed in the case of 1PA and the extension of the electronic conjugation. A pronounced bathochromic shift in the 2PA spectrum associated with a definite broadening of the 2PA band is obtained, whereas the 2PA cross-section values increase significantly in the spectral range of interest for biological application (700–1000 nm) as illustrated by octupolar compound **19d**; its 2PA cross-section value peaks at 2070 GM (800 nm) and remains superior to 1000 GM from 750 to 950 nm.

Figure 8 shows that the nature of the connector also plays an important role. Indeed, when comparing compounds **16b** and **17**, we observe that the replacement of a phenylene moiety by a less aromatic EDOT moiety in the conjugated arms significantly increases the 2PA cross-sections over the whole spectral range of interest. Hence, fluorophore **17**, which is also the more redshifted emitter of the series, maintains sizeable 2PA cross-sections in the whole 700–950 nm spectral range.

The introduction of a fluorenylene–vinylene in the conjugated arms also allows one to attain very high 2PA responses over a wide spectral range, with 2PA cross-sections superior to 1000 GM from 700 to 900 nm for fluorophore **20** (Figure 8). Octupolar compound **20**, which is the biggest derivative in the investigated series, is found to exhibit to the highest two-photon brightness ($\sigma_2\Phi^{max} \approx 2000$ GM).

### Bioapplication: Cellular Imaging

By taking advantage of the demonstrated brightness and polarity sensitivity of the series of octupolar fluorescent dyes, we decided to investigate their potential use as *in cellulo* fluorescent two-photon markers. Toward this aim, we selected the two hydrophilic chromophores that bear $SO_2CH_2CH_2OH$ peripheral groups, that is, octupolar compounds **15a**, **19f**, and one amphiphilic dissymmetrical derivative (**19g**) that bear two strong EW peripheral moieties ($SO_2CF_3$) and one hydrophilic one ($SO_2$-$CH_2$-$CH_2$-OH). These derivatives, which combine good fluorescence, significant 2PA response in the 700–900 nm region, and marked polarity sensitivity (with specific shift values higher than 17000 $cm^{-1}$) were thus suitable as two-photon markers and appeared to be promising probes for cellular imaging. We stress that, upon going from **15a** to **19f** and **19g**, the emission is nicely redshifted (Table 1) and the 2PA responses are further increased.

These dedicated dyes were then tested in 2PEF microscopic imaging of live cells and sensing of the polarity of cellular microenvironments. In each case, human embryonic kidney 293 cells (HEK293) were incubated with a 3 μM solution of the fluorescent dye for 1.5 h, then washed with phosphate-buffered saline (PBS) solution, and finally incubated in a culture-cell medium for one night to allow further cell growth. The obtained cover slips were analyzed with a confocal microscope and combined transmission and 2PEF images were acquired. λ-Scan experiments were also performed to determine the emission spectrum of the fluorophores in the cellular environment. We checked after each λ-scan experiment that the laser irradiation did not damage cells by combined transmission and 2PEF imaging, then compared the images to the previously acquired one. The three dyes were found to show good to excellent biocompatibility considering the shape and the number of observable cells in the transmission images. We observed that cells are grown to 80% confluency in the presence of compounds **15a** and **19f**. These two octupolar derivatives thus allow high cell viability. The dissymmetrical derivative **19g** appears to have slightly lower biocompatibility, because the cell adhesion on the cover slip after similar incubation time lessens. This slightly lower biocompatibility can possibly be ascribed to the presence of the fluorinated moiety.

2PEF images obtained when exciting at 750 or 780 nm (at which all fluorophores show significant 2PA responses) clearly reveal that these novel two-photon fluorescent probes penetrate into the cell, presumably through internalization or endocytosis mechanisms. When using compound **15a** as the two-photon probe, the dyes were mainly found in the cell cytoplasm and do not enter the nucleus as illustrated in Figure 9. In all imaging experiments, the probes were observed to display an intense 2PEF response, which demonstrates that they retain their excellent 2PA and photoluminescence properties in biological conditions. Moreover, the 2PEF images obtained after incubation with the three different hydrophilic fluorescent two-photon probes (**15a, 19f**, and **19g**), when using the same probe concentration and laser power for 2P excitation at the same wavelength, show relative intensities that match the 2P brightness ($\sigma_2\Phi$) of the different fluorescent dyes (i.e., 250, 268, and 120 GM at 750 nm in ethanol), which suggests that uptake ratios are similar for the three fluorescent dyes. The fluorescence intensities were further normalized to allow comparison of the emission spectra collected by means of λ-scan experiments (Figure 10). The three fluorescent dyes allow monitoring of cytoplasmic micropolarity in living cells: all three compounds display a broad emission spectrum with a maximum at 460, 510, and 520 nm for derivatives **15a**, **19f**, and **19g**, respectively. A comparison of these spectra and those ob-

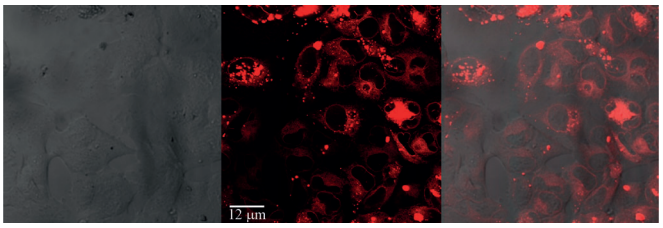


Figure 9. Transmission (left), 2PEF (middle, excited at 750 nm), and merged images (right) of HEK 293 cells labeled with hydrophilic fluorescent probe **15a.**

tained in solvents of varying polarity (Figure 10 bottom, see also the Supporting Information) reveals that the HEK293 cytoplasm behaves like a low-polarity environment. In the case of amphiphilic derivative **19g**, 2PEF images also clearly reveal brighter spots that suggest that the Y-shaped two-photon dye tends to accumulate in specific intracellular compartments, most likely lysosomes (Figure 11).

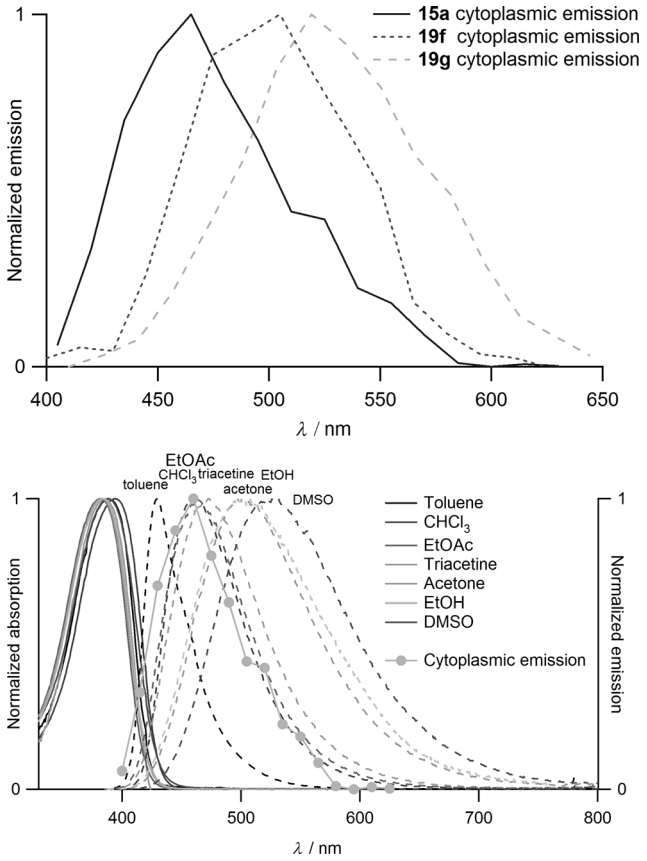


Figure 10. Top: emission spectra of fluorophores **15a**, **19f**, and **19g** in HEK 293 cytoplasm obtained from λ-scan experiments excited at 750 nm. Bottom: emission spectra of hydrophilic fluorescent probe **15a** in various environments.

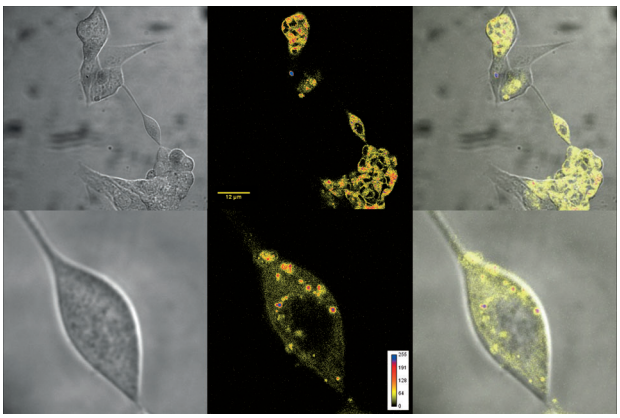

Figure 11. Transmission (left), 2PEF (middle, excited at 750 nm), and merged images (right) of HEK 293 cells labeled with amphiphilic fluorescent probe **19g**.

## Conclusion

A series of octupolar fluorophores built from a TPA core and that bear different EW peripheral groups and conjugated spacers has been synthesized. Structure–property relationships were derived from the comprehensive study of the absorption, photoluminescence, and two-photon absorption properties of these compounds. The low-energy transition is correlated to a core-to-periphery intramolecular charge-transfer phenomenon that leads to intense absorption in the visible near-UV blue-visible range. In addition, thanks to an efficient coupling of the branches through the TPA core, all derivatives show an additional intense 2PA band located at higher energy than that which corresponds to the lowest excited state. As a result, all derivatives exhibit significant 2PA responses in the spectral range of interest for biomedical applications, with two broad bands in the 700–900 nm region. All derivatives were found to show intense photoluminescence in low- to medium-polarity environments (with fluorescence quantum yields ranging from 0.5 to 0.9)

Absorption, 2PA, and emission can be tuned by playing on the structural parameters and taking advantage of the highly modular and flexible synthesis approach. In analogy with quadrupolar derivatives designed from a comparable modular approach, increasing the electron-withdrawing strength of the end groups or the conjugated spacer length and replacing a triple bond linker with a double bond induce a redshift of the emission, and both an enhancement and broadening of the 2PA responses in the 700–1000 nm spectral range. As a result, a number of octupolar derivatives (i.e., those that combine powerful EW peripheral groups and with the longest conjugated spacers) exhibit large 2PA responses (superior to 1000 GM over the whole 700–900 nm range with up to 2100 GM peak 2PA response).

Excitation localization on the dipolar branches occurs after absorption prior to emission, thereby leading to highly polar emissive excited states. Photoluminescence of these octupolar chromophores is thus highly sensitive to the polarity of the environment. All compounds display a strong positive solvatochromic behavior that fits the Lippert–Mataga relationship, thereby allowing us to quantify (by means of the slope or specific shift values) the sensitivity to polarity. Interestingly, the probe sensitivity was found to depend strongly on the strength of the peripheral groups and on the nature of the conjugated spacer, with specific shift values ranging between 15000 and 27500 $cm^{-1}$ (i.e., much higher, for instance, than that reported for a standard probe such as Nile red: 1700 $cm^{-1}$). The larger sensitivity is obtained for elongated derivatives with a triple bond in the conjugated spacer, whereas replacement of a phenyl moiety with a less aromatic EDOT (which efficiently redshifts the emission) results in a marked decrease in sensitivity (thus leading to a specific shift that is almost twice as small).

Finally, three more hydrophilic derivatives (either octupolar or dissymmetrical) that combine significant luminescence, 2PA in the 700–850 region, and polarity sensitivity were tested as two-photon markers for cell imaging by

means of 2PEF microscopy. These two-photon probes were shown to be biocompatible and to retain their 2PA and luminescence properties under biological conditions. Indeed, 2PEF images show that these probes enter the cells and label the cytoplasm. Furthermore, their environment-dependent emission reveals intracellular media of low polarity. These derivatives open a promising route to the design of organelle-selective, two-photon probes. Further functionalization with targeting moieties will be studied as well as their potential use as polarity sensors for (nano)materials.

## Experimental Section

*Synthetic Procedures*

All air- or water-sensitive reactions were carried out under argon. Solvents were generally dried and distilled prior to use. Reactions were monitored by thin-layer chromatography on Merck silica gel or neutral aluminum oxide 60 $F_{254}$ precoated aluminum sheets. Column chromatography: Merck silica gel Si 60 (40–63 μm, 230–400 mesh). Melting points were determined with an Electrothermal IA9300 digital melting point instrument. NMR: Bruker AM 200 ($^1$H: 200.13 MHz), AM250 ($^1$H: 250.13 MHz, $^{13}$C: 62.90 MHz, $^{31}$P: 101.25 MHz), ARX 200 ($^1$H: 200.13 MHz, $^{13}$C: 50.32 MHz), or Avance AV 300 ($^1$H: 300.13 MHz, $^{13}$C: 75.48 MHz, $^{19}$F: 282.38 MHz, $^{31}$P: 121.50 MHz), in $CDCl_3$ solutions; $^1$H chemical shifts ($\delta$) are given in ppm relative to TMS as internal standard, $J$ values in Hz, $^{13}$C chemical shifts relative to the central peak of $CDCl_3$ at $\delta = 77.0$ ppm, $^{31}$P relative to $H_3PO_4$ as external standard, and $^{19}$F relative to $CFCl_3$ as internal standard. High- and low-resolution mass spectra measurements were performed at the Centre Régional de Mesures Physiques de l'Ouest (C.R.M.P.O., Rennes) with a Micromass MS/MS ZAB-Spec TOF instrument with EBE TOF geometry; liquid secondary-ion mass spectrometry (LSIMS) at 8 kV with $Cs^+$ in *m*-nitrobenzyl alcohol (*m*NBA); $ES^+$ (electrospray ionization, positive mode) at 4 kV; electron ionization (EI) at 70 eV. Elemental analyses were performed at I.C.S.N.–C.N.R.S. (Gif-sur-Yvette, France) or at the C.R.M.P.O. Phosphonates **1a**,**b** and **5** were prepared analogously to Ref. [29] and Ref. [30], respectively. Compounds **3a**,**b**,[9j] **6**,[17] **8a**,[9j] **12**,[18] **14**,[19] **18a**,[20] **19f**,[27] and **19g**,[27] were synthesized according to the respective literature procedures.

*1-Iodo-4-{(1E)-2-[4-(octylsulfonyl)phenyl]ethenyl}benzene (**2a**)*

NaH (273 mg, 60% dispersion in mineral oil) was added to a solution of **1a** (1.702 g, 4.208 mmol) and 4-iodobenzaldehyde (1.057 g, 4.556 mmol) in anhydrous THF (16 mL). The mixture was stirred at 20 °C for 15 h. After the addition of water, the product was extracted with $CH_2Cl_2$ and was then purified by column chromatography (heptane/$CH_2Cl_2$ 30:70) to yield **2a** (1.242 g, 61%). M.p. 158–159 °C; $^1$H NMR (200.13 MHz, $CDCl_3$): $\delta = 7.88$ and 7.66 (AA′XX′, $J$(A,X) = 8.5 Hz, 4H), 7.72 and 7.27 (AA′XX′, $J$(A,X) = 8.5 Hz, 4H), 7.15 (s, 2H), 3.09 (m, 2H), 1.72 (m, 2H), 1.24 (m, 10H), 0.86 ppm (t, $J = 5.7$ Hz, 3H); $^{13}$C NMR (50.32 MHz, $CDCl_3$): $\delta = 142.1$, 137.8, 137.6, 135.7, 131.2, 128.4, 127.2, 126.9, 94.0, 56.3, 31.5, 29.6, 28.84, 28.77, 22.6, 22.4, 14.0 ppm; HRMS (LSIMS$^+$, mNBA): $m/z$ calcd for $C_{22}H_{28}IO_2S$: 483.0855 $[M+H]^+$; found: 483.0864.

*1-Iodo-4-[(1E)-2-{4-[(trifluoromethyl)sulfonyl]phenyl}ethenyl]benzene (**2b**)*

*t*BuOK (48 mg, 428 μmol) was added to a solution of **1b** (100 mg, 278 μmol) and 4-iodobenzaldehyde (99 mg, 427 μmol) in anhydrous $CH_2Cl_2$ (5 mL). The mixture was stirred at 20 °C for 15 h. After the addition of water (10 mL) and extraction with $CH_2Cl_2$, the crude product was purified by column chromatography ($CH_2Cl_2$/heptane 30:70) to yield **2b** (63 mg, 52%). M.p. 142–143 °C; $^1$H NMR (200.13 MHz, $CDCl_3$): $\delta = 8.00$ and 7.74 (AA′XX′, $J$(A,X) = 8.6 Hz, 4H), 7.73 and 7.29 (AA′XX′, $J$(A,X) = 8.3 Hz, 4H), 7.25 (d, $J = 16.4$ Hz, 1H), 7.13 ppm (d, $J = 16.4$ Hz, 1H); $^{13}$C NMR (75.47 MHz, $CDCl_3$): $\delta = 145.3$, 138.0, 135.4, 133.3, 131.3, 129.2, 128.7, 127.4, 126.7, 119.8 (q, $J = 325.8$ Hz), 94.8 ppm; HRMS (EI): $m/z$ calcd for $C_{15}H_{10}F_3IO_2S$: 437.9398 $[M^+\cdot]$; found: 437.9374.

*4-[(1E)-2-{4-[(Trifluoromethyl)sulfonyl]phenyl}ethenyl]benzaldehyde (**4a**)*

Air was removed from a solution of **3b**[9j] (630.4 mg, 2.18 mmol), *p*-vinylbenzaldehyde[16] (432.2 mg, 3.17 mmol), and $K_2CO_3$ (452 mg, 3.27 mmol) in anhydrous DMF (10 mL) by blowing argon for 30 min. Then $n$Bu$_4$NCl (606 mg, 2.18 mmol), $PPh_3$ (57.2 mg, 0.218 mmol), and $Pd(OAc)_2$ (24.5 mg, 0.109 mmol) were added, and the mixture was stirred at 110 °C for 10 h. The solvent was removed by distillation under vacuum. After washing with heptane, the crude product was purified by column chromatography (heptane/$CH_2Cl_2$ 40:60) to yield **4a** (190.5 mg, 26%). M.p. 161–162 °C; $^1$H NMR (200.13 MHz, $CDCl_3$): $\delta = 10.04$ (s, 1H), 8.04 and 7.80 (AA′XX′, $J$(A,X) = 8.5 Hz, 4H), 7.93 and 7.72 (AA′XX′, $J$(A,X) = 8.3 Hz, 4H), 7.40 (d, $J = 16.4$ Hz, 1H), 7.29 ppm (d, $J = 16.4$ Hz, 1H); $^{13}$C NMR (75.47 MHz, $CDCl_3$): $\delta = 191.4$, 144.8, 141.7, 136.3, 132.9, 131.3, 130.3, 129.8, 129.1, 127.8, 127.6, 119.8 ppm (q, $J = 325.9$ Hz); HRMS (EI): $m/z$ calcd for $C_{16}H_{11}F_3O_3S$: 340.0381 $[M^+\cdot]$; found: 340.0380; elemental analysis calcd (%) for $C_{16}H_{11}F_3O_3S$ (340.32): C 56.47, H 3.26, S 9.42; found: C 56.68, H 3.48, S 9.42.

*1-Ethenyl-4-[(1E)-2-{4-[(trifluoromethyl)sulfonyl]phenyl}ethenyl]benzene (**4b**)*

*t*BuOK (70 mg, 624 μmol) was added to a solution of **4a** (68.8 mg, 202 μmol) and methyltriphenylphosphonium iodide (162.1 mg, 401 μmol) in anhydrous $CH_2Cl_2$ (4.5 mL). The mixture was stirred at 20 °C for 3 h. After filtration through Celite ($CH_2Cl_2$), the solvent was evaporated, and the crude product was purified by column chromatography (heptane/$CH_2Cl_2$ 70:30) to yield of **4b** (34.8 mg, 51%). M.p. 138.5–139.5 °C; $^1$H NMR (200.13 MHz, $CDCl_3$): $\delta = 8.00$ and 7.74 (AA′XX′, $J$(A,X) = 8.5 Hz, 4H), 7.53 and 7.44 (AA′XX′, $J$(A,X) = 8.5 Hz, 4H), 7.32 (d, $J = 16.3$ Hz, 1H), 7.14 (d, $J = 16.3$ Hz, 1H), 6.74 (dd, $J = 17.6$, 10.9 Hz, 1H), 5.81 (dd, $J = 17.6$, 0.7 Hz, 1H), 5.31 ppm (dd, $J = 10.9$, 0.7 Hz, 1H); $^{13}$C NMR (75.47 MHz, $CDCl_3$): $\delta = 145.8$, 138.4, 136.2, 135.3, 134.1, 131.2, 128.9, 127.4, 127.3, 126.8, 125.7, 119.9 (q, $J = 326.1$ Hz), 114.8 ppm; HRMS (EI): $m/z$ calcd for $C_{17}H_{13}F_3O_2S$: 338.0588 $[M^+\cdot]$; found: 338.0589; elemental analysis calcd (%) for $C_{17}H_{13}F_3O_2S$ (338.35): C 60.35, H 3.87, S 9.48; found: C 60.53, H 3.82, S 9.49.

*2-Iodo-5-[(1E)-2-{4-[(trifluoromethyl)sulfonyl]phenyl}ethenyl]-3,4-ethylenedioxythiophene (**7**)*

*t*BuOK (232 mg, 2.072 mmol) was added to a solution of **6**[17] (498 mg, 1.382 mmol) and **1b** (450 mg, 1.520 mmol) in anhydrous $CH_2Cl_2$. The reaction mixture was stirred in the dark at 20 °C for 15 h. Then the mixture was filtered through Celite, the solvent was evaporated, and the crude product was purified by column chromatography (heptane/$CH_2Cl_2$, gradient from 80:20 to 60:40) to yield **7** (302 mg, 43%). M.p. 171–172 °C; $^1$H NMR (200.13 MHz, $CDCl_3$): $\delta = 7.94$ and 7.65 (AA′XX′, $J$(A,X) = 8.6 Hz, 4H), 7.30 (d, $J = 16.1$ Hz, 1H), 6.79 (d, $J = 16.1$ Hz, 1H), 4.32 ppm (s, 4H); $^{13}$C NMR (75.47 MHz, $CDCl_3$): $\delta = 145.7$, 144.7, 140.0, 131.2, 128.3, 126.8, 123.4, 122.9, 121.0, 119.9 (q, $J = 326$ Hz), 65.2, 64.9, 51.7 ppm; $^{19}$F NMR (282.37 MHz, $CDCl_3$): $\delta = -78.47$ ppm; HRMS ($ES^+$, MeOH): $m/z$ calcd (%) for $C_{15}H_{10}O_4F_3NaIS_2$: 524.8915 $[M+Na]^+$; found: 524.8922; elemental analysis calcd (%) for $C_{15}H_{10}O_4F_3IS_2$ (525.26): C 35.87, H 2.01, S 12.77; found: C 36.09, H 2.01, S 12.47.

*7-Iodo-9,9-dioctyl-9H-fluorene-2-carboxaldehyde (**8b**)*

A solution of *n*-butyllithium 2.5 M in hexanes (2.19 mL, 5.481 mmol) was added dropwise to a solution of **8a**[9j] (3.5 g, 5.22 mmol) in anhydrous diethyl ether (40 mL) at −78 °C. The reaction mixture was stirred at −78 °C for 30 min, then allowed to cool to 20 °C, and stirred for 30 min. Thereafter the mixture was cooled at −78 °C and DMF was added (0.64 g, 8.73 mmol), then it was allowed to cool to room temperature for 15 h. HCl (2 N, 25 mL) was added and the organic layer extracted. The aqueous layer was washed with diethyl ether (50 mL). The collected organic layers were dried ($Na_2SO_4$). After evaporation of the solvents, the crude product was purified by column chromatography (heptane/$CH_2Cl_2$, gradi-

ent from 75:25 to 65:35) to yield **8b** (0.8 g, 27%). $^1$H NMR (200.13 MHz, $CDCl_3$): $\delta$ = 10.06 (s, 1H), 7.83 (m, 3H), 7.70 (m, 2H), 7.51 (d, $J$ = 8.4 Hz, 1H), 3.95 (m, 4H), 1.26–1.03 (m, 24H), 0.83 (t, $J$ = 7.3 Hz, 6H), 0.56 ppm (m, 4H); $^{13}$C NMR (50.32 MHz, $CDCl_3$): $\delta$ = 191.9, 154.3, 150.8, 146.3, 139.1, 136.2, 135.7, 132.3, 130.3, 123.0, 122.4, 120.0, 94.8, 55.4, 39.9, 31.7, 29.7, 29.3, 29.0, 29.0, 23.6, 22.5, 14.0 ppm; HRMS (ES$^+$, MeOH): $m/z$ calcd for $C_{32}H_{45}OINa$: 595.2413 [$M$+Na]$^+$; found: 595.2410.

*1-Bromo-4-[(nonafluorobutyl)thio]benzene (**10b**)*

NaH (305 mg, 12.69 mmol) was added to a solution of **10a** (2 g, 10.58 mmol) in anhydrous DMF (2 mL) cooled in an ice water bath. The mixture was stirred for 1 h at 20°C. Then 1-iodononafluorobutane (4.026 g, 11.64 mmol) was added dropwise, and the solution was stirred for 2 h at 20°C. The solvent was removed by distillation under vacuum. After adding water, the product was extracted with EtOAc, and the residue was purified by column chromatography (heptane) to yield **10b** (3.95 g, 92%).[31] $^1$H NMR (200.13 MHz, $CDCl_3$): $\delta$ = 7.55 and 7.51 ppm (AA′XX′, $J$(A,X) = 8.8 Hz, 4H).

*1-Bromo-4-[(nonafluorobutyl)sulfonyl]benzene (**11**)*

A solution of **10b** (2 g, 4.913 mmol) in glacial acetic acid (80 mL) and 35% aqueous $H_2O_2$ (27 mL) was heated to reflux for 3 h. After cooling, the product was extracted with $CH_2Cl_2$, and the organic layers were washed first with a saturated solution of $NaHCO_3$ (three times) then with water (three times). After evaporation of solvent, the residue was purified by column chromatography (heptane) to yield **11** (1.531 g, 71%). M.p. 57–58°C (Ref. [31], 56°C); $^1$H NMR (200.13 MHz, $CDCl_3$): $\delta$ = 7.90 and 7.84 ppm (AA′XX′, $J$(A,X) = 8.9 Hz, 4H).

*2-({4-[(Trimethylsilyl)ethynyl]phenyl}sulfonyl)ethanol (**13a**)*

Air was removed from a solution of **12**[18] (1.0053 g, 3.79 mmol) in toluene/$Et_3N$ (5:1, 10 mL) by blowing argon for 20 min. Then CuI (14.4 mg, 75.8 μmol), [$Pd(PPh_3)_2Cl_2$] (53.2 mg, 75.8 μmol), and ethynyltrimethylsilane (810 μL, 5.688 mmol) were added. The mixture was heated for 16 h at 40°C. The solvents were evaporated, and the residue was purified by column chromatography ($CH_2Cl_2$/EtOAc 90:10) to yield **13a** (1.024 g, 96%). M.p. 93–94°C; $^1$H NMR (200.13 MHz, $CDCl_3$): $\delta$ = 7.86 and 7.65 (AA′XX′, $J$(A,X) = 8.4 Hz, 4H), 3.99 (m, 2H), 3.34 (t, $J$ = 5.3 Hz, 2H), 2.66 (t, $J$ = 6.5 Hz, 1H), 0.27 ppm (s, 9H); $^{13}$C NMR (75.47 MHz, $CDCl_3$): $\delta$ = 138.1, 132.6, 129.3, 128.8, 102.7, 99.6, 58.2, 56.2, 0.0 ppm; HRMS (EI): $m/z$ calcd for $C_{13}H_{18}O_3SiS$: 282.07459 [$M^+$·]; found: 282.0746; elemental analysis calcd (%) for $C_{13}H_{18}O_3SiS$ (282.44): C 55.28, H 6.42, S 11.35; found: C 55.34, H 6.35, S 11.25.

*2-[(4-Ethynylphenyl)sulfonyl]ethanol (**13b**)*

NaOH (1M, 9.5 mL, 9.5 mmol) was added to a solution of **13a** (1.004 g, 3.55 mmol) in THF (19 mL). The mixture was stirred for 15 min at 20°C. THF was removed, then the product was extracted by $CH_2Cl_2$, and the residue was purified by column chromatography ($CH_2Cl_2$/EtOAc 90:10) to yield **13b** (709 mg, 95%). M.p. 73–74°C; $^1$H NMR (200.13 MHz, $CDCl_3$): $\delta$ = 7.90 and 7.69 (AA′XX′, $J$(A,X) = 8.6 Hz, 4H), 4.02 (m, 2H), 3.36 (t, $J$ = 5.3 Hz, 2H), 3.31 (s, 1H), 2.65 ppm (t, $J$ = 6.4 Hz, 1H); $^{13}$C NMR (50.32 MHz, $CDCl_3$): $\delta$ = 138.7, 132.9, 128.2, 127.9, 81.6, 81.6, 58.2, 56.2 ppm; HRMS (EI): $m/z$ calcd for $C_{10}H_{10}O_3S$: 210.03507 [$M^+$·]; found: 210.0360; elemental analysis calcd (%) for $C_{10}H_{10}O_3S$ (210.25): C 57.13, H 4.79, S 15.25; found: C 57.21, H 4.86, S 15.66.

*Tris{4-[(trimethylsilyl)ethynyl]phenyl}amine (**14b**)*

Air was removed from a solution of **14a**[19] (1.0 g, 1.605 mmol) in toluene/$Et_3N$ (5:1, 8 mL) by blowing argon for 20 min. Then CuI (37 mg, 0.194 mmol), [$Pd(PPh_3)_2Cl_2$] (68 mg, 0.097 mmol), and ethynyltrimethylsilane (1.15 mL, 8.14 mmol) were added. The reaction mixture was heated at 40°C for 3 h. The solvent was evaporated under vacuum, and the crude product was purified by column chromatography (heptane/$CH_2Cl_2$ 80:20) to yield **14b** (820 mg, 96%). M.p. 172–175°C; $^1$H NMR (200.13 MHz, $CDCl_3$): $\delta$ = 7.34 and 6.95 (AA′XX′, $J$(A,X) = 8.5 Hz, 12H), 0.24 ppm (s, 27H); $^{13}$C NMR (50.32 MHz, $CDCl_3$): $\delta$ = 146.8, 133.1, 123.8, 117.8, 104.8, 93.9, 0.0 ppm; HRMS (LSIMS$^+$, mNBA): $m/z$ calcd for $C_{33}H_{39}NSi_3$: 533.2390 [$M^+$·]; found: 533.2390.

*Tris[4-(ethynylphenyl)]amine (**14c**)*

NaOH (1M, 30 mL) was added to a solution of **14b** (2.33 g, 4.36 mmol) in THF (30 mL). The reaction mixture was stirred for 35 h at 20°C. The solvent was evaporated, the product was extracted with $CH_2Cl_2$, and the organic layer washed with water. The residue was purified by column chromatography ($CH_2Cl_2$/heptane, gradient from 10:90 to 15:85) to yield **14c** (1.20 g, 87%). M.p. 113–114°C (Ref. [32] 110–112°C); $^1$H NMR (200.13 MHz, $CDCl_3$): $\delta$ = 7.38 and 7.02 (AA′XX′, $J$(A,X) = 8.9 Hz, 12H), 3.05 ppm (s, 3H); $^{13}$C NMR (50.32 MHz, $CDCl_3$): $\delta$ = 147.0, 133.3, 123.9, 116.8, 83.4, 76.97 ppm; HRMS (LSIMS$^+$, mNBA): $m/z$ calcd for $C_{24}H_{15}N$: 317.12045 [$M^+$·]; found: 317.1212; elemental analysis calcd (%) for $C_{24}H_{15}N$ (317.39): C 90.82, H 4.76, N 4.41; found: C 90.39, H 4.93, N 4.28.

*Tris[4-({4-[(2-hydroxyethyl)sulfonyl]phenyl}ethynyl)phenyl]amine (**15a**)*

Air was removed from a solution of **14a** (182 mg, 0.288 mmol) and **13b** (243 mg, 1.152 mmol) in toluene/$Et_3N$ (5:1; 9 mL) by blowing argon for 20 min. Then CuI (3.3 mg, 17.3 μmol) and [$Pd(PPh_3)_2Cl_2$] (12.1 mg, 17.3 μmol) were added. The reaction mixture was stirred at 40°C for 15 h. The solvents were removed, and the crude product was purified by column chromatography ($CH_2Cl_2$/EtOH 95:5) to yield **15a** (251 mg, 78%). M.p. 146°C; $^1$H NMR (200.13 MHz, $CDCl_3$): $\delta$ = 7.91 and 7.70 (AA′XX′, $J$(A,X) = 8.4 Hz, 12H), 7.48 and 7.11 (AA′XX′, $J$(A,X) = 8.6 Hz, 12H), 4.03 (m, 6H), 3.38 (m, 6H), 2.75 ppm (s, 3H); $^{13}$C NMR (75.47 MHz, $CDCl_3$): $\delta$ = 147.1, 137.8, 133.2, 132.2, 129.6, 128.0, 124.1, 117.1, 93.6, 87.7, 58.3, 56.3 ppm; HRMS (ES$^+$, MeOH): $m/z$ calcd for $C_{48}H_{39}NO_9NaS_3$: 892.1685 [$M$+Na]$^+$; found: 892.1675.

*Tris(4-{[4-(octylsulfonyl)phenyl]ethynyl}phenyl)amine (**15b**)*

Air was removed from a solution of **14b** (55.5 mg, 104 μmol) and **3a**[9j] (125 mg, 375 μmol) in toluene/$Et_3N$ (5:1, 6 mL) by blowing argon for 20 min. Then $PPh_3$ (6.6 mg, 25.2 μmol), [$Pd_2(dba)_3$] (2.9 mg, 3.2 μmol), CuI (1.7 mg, 8.9 μmol), and tetrabutylammonium fluoride (1M solution in THF, 312 μL) were added. The reaction mixture was heated at 35°C for 22 h. The solvent was removed, and the crude product was purified by column chromatography (heptane/$CH_2Cl_2$, gradient from 50:50 to 40:60) to yield **15b** (73 mg, 65%). M.p. 72–74°C; $^1$H NMR (200.13 MHz, $CDCl_3$): $\delta$ = 7.88 and 7.68 (AA′XX′, $J$(A,X) = 8.4 Hz, 12H), 7.48 and 7.12 (AA′XX′, $J$(A,X) = 8.6 Hz, 12H), 3.10 (m, 6H), 1.71 (m, 6H), 1.35 (m, 6H), 1.24 (m, 24H), 0.87 ppm (t, $J$ = 6.3 Hz, 9H); $^{13}$C NMR (50.32 MHz, $CDCl_3$): $\delta$ = 147.1, 138.1, 133.1, 132.0, 129.1, 128.1, 124.1, 117.2, 93.2, 87.8, 56.3, 31.6, 28.9, 28.8, 28.2, 22.6, 22.5, 14.0 ppm; HRMS (LSIMS$^+$, mNBA): $m/z$ calcd for $C_{66}H_{75}NO_6S_3$: 1073.4756 [$M^+$·]; found: 1073.4765; elemental analysis calcd (%) for $C_{66}H_{75}NO_6S_3$ (1074.50): C 73.77, H 7.04, N 1.30, S 8.93; found: C 73.31, H 7.21, N 1.66, S 8.65.

*Tris[4-({4-[(trifluoromethyl)sulfonyl]phenyl}ethynyl)phenyl]amine (**15c**)*

Air was removed from a solution of **14b** (90.6 mg, 170 μmol) and **3b**[9j] (180.8 mg, 625 μmol) in toluene/$Et_3N$ (5:1, 6 mL) by blowing argon for 20 min. Then $PPh_3$ (12.6 mg, 48 μmol), [$Pd_2(dba)_3$] (5.9 mg, 6.4 μmol), CuI (2.0 mg, 10.5 μmol), and tetrabutylammonium fluoride (1M solution in THF, 510 μL) were added. The reaction mixture was heated at 35°C for 22 h. The solvent was evaporated, and the crude product was purified by column chromatography (heptane/$CH_2Cl_2$ 50:50) to yield **15c** (134.4 mg, 84%). M.p. 255–257°C; $^1$H NMR (200.13 MHz, $CDCl_3$): $\delta$ = 8.02 and 7.76 (AA′XX′, $J$(A,X) = 8.3 Hz, 12H), 7.50 and 7.14 ppm (AA′XX′, $J$(A,X) = 8.6 Hz, 12H); $^{13}$C NMR (50.32 MHz, $CDCl_3$): $\delta$ = 147.3, 133.4, 132.4, 132.3, 130.7, 129.7 (d, $J$ = 1.6 Hz), 124.2, 119.7 (q, $J$ = 325.9 Hz), 116.9, 95.6, 87.5 ppm; $^{19}$F NMR (282.38 MHz, $CDCl_3$): $\delta$ = −78.23 ppm; HRMS (LSIMS$^+$, mNBA): $m/z$ calcd for $C_{45}H_{24}F_9NO_6S_3$: 941.0622 [$M^+$·]; found: 941.0618; elemental analysis calcd (%) for $C_{45}H_{24}F_9NO_6S_3$ (941.85): C 57.39, H 2.57, N 1.49, S 10.21; found: C 57.19, H 2.78, N 1.39, S 10.22.

*Tris[4-({4-[(nonafluorobutyl)sulfonyl]phenyl}ethynyl)phenyl]amine (**15d**)*

Air was removed from a solution of **14c** (41.7 mg, 0.131 mmol) and **11** (230.8 mg, 0.525 mmol) in toluene/$Et_3N$ (5:1, 7.5 mL) by blowing argon for 20 min. Then $PPh_3$ (10.3 mg, 39 μmol), CuI (1.5 mg, 7.88 μmol), and $[Pd_2(dba)_3]$ (3.6 mg, 3.94 μmol) were added. The reaction mixture was heated at 35 °C for 20 h. After evaporation of solvents, the residue was purified by column chromatography (heptane/$CH_2Cl_2$ 50:50) to yield **15d** (85 mg, 47 %). M.p. 174–175 °C; $^1$H NMR (300.13 MHz, $CDCl_3$): $\delta$ = 8.00 and 7.75 (AA′XX′, $J$(A,X) = 8.5 Hz, 12H), 7.49 and 7.12 ppm (AA′XX′, $J$(A,X) = 8.6 Hz, 12H); $^{19}$F NMR (282.35 MHz, $CDCl_3$): $\delta$ = −80.65 (m, 9F), −111.44 (t, $J$ = 13.8 Hz, 6F), −120.77 (m, 6F), −125.91 ppm (m, 6F); HRMS (ES$^+$, MeOH/$CH_2Cl_2$ 95:5): $m/z$ calcd for $C_{54}H_{24}NO_6F_{27}NaS_3$: 1414.0232 $[M+Na]^+$; found: 1414.0199.

*Tris{4-[(4-{(1E)-2-[4-(octylsulfonyl)phenyl]ethenyl}phenyl)ethynyl]phenyl}amine (**16a**)*

Air was removed from a solution of **14b** (100.1 mg, 187 μmol) and **2a** (321.6 mg, 656 μmol) in toluene/$Et_3N$ (5:1, 6 mL) by blowing argon for 20 min. Then $PPh_3$ (14.6 mg, 45 μmol), $[Pd_2(dba)_3]$ (5.2 mg, 5.6 μmol), CuI (2.1 mg, 11.2 μmol), and tetrabutylammonium fluoride (1 M solution in THF, 562 μL) were added. The reaction mixture was stirred at 20 °C for 65 h. The solvents were removed, and the residue was purified by column chromatography (heptane/$CH_2Cl_2$, gradient from 30:70 to 0:100) to yield **16a** (230 mg, 89 %). M.p. 118–120 °C; $^1$H NMR (200.13 MHz, $CDCl_3$): $\delta$ = 7.89 and 7.68 (AA′XX′, $J$(A,X) = 8.5 Hz, 12H), 7.54 (s, 12H), 7.46 and 7.10 (AA′XX′, $J$(A,X) = 8.7 Hz, 12H), 7.26 (d, $J$ = 16.4 Hz, 3H), 7.15 (d, $J$ = 16.4 Hz, 3H), 3.10 (m, 6H), 1.73 (m, 6H), 1.24 (m, 30H), 0.86 ppm (t, $J$ = 6.5 Hz, 9H); $^{13}$C NMR (50.32 MHz, $CDCl_3$): $\delta$ = 146.7, 142.4, 137.6, 136.0, 132.8, 131.9, 131.7, 128.6, 127.3, 127.0, 126.9, 124.0, 123.5, 117.8, 90.8, 89.3, 56.4, 31.6, 28.94, 28.87, 28.3, 22.7, 22.5, 14.0 ppm; HRMS (LSIMS$^+$, mNBA): $m/z$ calcd for $C_{90}H_{93}NO_6S_3$: 1379.6165 $[M^+\cdot]$; found: 1379.6172; elemental analysis calcd (%) for $C_{90}H_{93}NO_6S_3$ (1380.91): C 78.28, H 6.79, N 1.01; found: C 78.35, H 6.83, N 0.96.

*Tris[4-({4-[(1E)-2-{4-[(trifluoromethyl)sulfonyl]phenyl}ethenyl]phenyl}ethynyl)phenyl]amine (**16b**)*

Air was removed from a solution of **14c** (72.4 mg, 0.228 mmol) and **2b** (328 mg, 0.748 mmol) in toluene/$Et_3N$ (5:1, 13 mL). Then $PPh_3$ (17.9 mg, 68.4 μmol), CuI (2.6 mg, 13.7 μmol), and $[Pd_2(dba)_3]$ (6.3 mg, 6.8 μmol) were added. The reaction mixture was heated at 35 °C for 15 h. After removing solvents, the residue was purified by column chromatography (heptane/$CH_2Cl_2$, gradient from 50:50 to 25:75) to yield **16b** (267 mg, 94 %). M.p. 139–141 °C; $^1$H NMR (200.13 MHz, $CDCl_3$): $\delta$ = 8.01 and 7.76 (AA′XX′, $J$(A,X) = 8.4 Hz, 12H), 7.55 (s, 12H), 7.46 and 7.10 (AA′XX′, $J$(A,X) = 8.5 Hz, 12H), 7.33 (d, $J$ = 16.3 Hz, 3H), 7.16 ppm (d, $J$ = 16.3 Hz, 3H); $^{13}$C NMR (75.47 MHz, $CDCl_3$): $\delta$ = 146.8, 145.5, 135.6, 133.6, 132.9, 132.0, 131.3, 129.2, 127.4, 127.1, 126.6, 124.1, 124.0, 119.8 (q, $J$ = 326.2 Hz), 117.8, 91.1, 89.3 ppm; $^{19}$F NMR (282.35 MHz, $CDCl_3$): $\delta$ = −78.39 ppm; HRMS (LSIMS$^+$, mNBA): $m/z$ calcd for $C_{69}H_{42}F_9NO_6S_3$: 1247.2031 $[M^+\cdot]$; found: 1247.1990; elemental analysis calcd (%) for $C_{69}H_{42}F_9NO_6S_3$ (1248.29): C 66.39, H 3.39, N 1.12, S 7.71; found: C 66.09, H 3.46, N 0.75, S 7.77.

*Tris[4-({5-[(1E)-2-{4-[(trifluoromethyl)sulfonyl]phenyl}ethenyl]-3,4-ethylenedioxythien-2-yl}ethynyl)phenyl]amine (**17**)*

The reaction of **14c** (22 mg, 69 μmol) with **7** (121 mg, 241 μmol) was as described for **16b**, for 13 h at 40 °C, with subsequent purification by column chromatography (heptane/$CH_2Cl_2$, gradient from 30:70 to 0:100) to afford **17** (84 mg, 84 %). M.p. 120–121 °C; $^1$H NMR (300.13 MHz, $CDCl_3$): $\delta$ = 7.95 and 7.66 (AA′XX′, $J$(A,X) = 8.4 Hz, 12H), 7.42 and 7.05 (AA′XX′, $J$(A,X) = 8.5 Hz, 12H), 7.34 (d, $J$ = 16.1 Hz, 3H), 6.88 (d, $J$ = 16.1 Hz, 3H), 4.34 ppm (s, 12H); $^{13}$C NMR (75.47 MHz, $CDCl_3$): $\delta$ = 146.7, 145.7, 144.2, 140.4, 132.7, 131.2, 129.0, 128.3, 126.9, 124.0, 123.0, 122.0, 119.9 (q, $J$ = 325.9 Hz), 117.5, 116.8, 98.3, 80.1, 65.1, 64.8 ppm; $^{19}$F NMR (282.37 MHz, $CDCl_3$): $\delta$ = −78.34 ppm; HRMS (LSIMS, mNBA): $m/z$ calcd for $C_{69}H_{42}NO_{12}F_9S_6$: 1439.08876 $[M^+\cdot]$; found: 1439.0885.

*Tris(4-ethenylphenyl)amine (**18b**)*

Sodium hydride (0.80 g, 33.398 mmol) was added to a solution of **18a**[20] (1.1 g, 3.339 mmol) and methyltriphenylphosphonium iodide (10.79 g, 26.72 mmol) in anhydrous THF (25 mL). The reaction mixture was stirred for 15 h at 20 °C. After filtration through Celite, the crude product was purified by column chromatography ($CH_2Cl_2$) to yield **18b** (1.07 g, 99 %). M.p. 81–82 °C; $^1$H NMR (200.13 MHz, $CDCl_3$): $\delta$ = 7.36 and 7.11 (AA′XX′, $J$(A,X) = 8.6 Hz, 12H), 6.73 (dd, $J$ = 17.6, 10.9 Hz, 3H), 5.72 (d, $J$ = 17.6 Hz, 3H), 5.23 ppm (d, $J$ = 10.9 Hz, 3H); $^{13}$C NMR (75.47 MHz, $CDCl_3$): $\delta$ = 147.0, 136.2, 132.4, 127.1, 124.1, 112.4 ppm; HRMS (EI): $m/z$ calcd for $C_{24}H_{21}N$: 323.1659 $[M^+\cdot]$; found: 323.1659.

*Tris(4-{(1E)-2-[4-(octylsulfonyl)phenyl]ethenyl}phenyl)amine (**19a**)*

*t*BuOK (151.5 mg, 1.35 mmol) was added to a solution of tris(4-formylphenyl)amine[20] (**18a**) (98.8 mg, 0.3 mmol) and **1a** (400.5 mg, 0.99 mmol) in anhydrous $CH_2Cl_2$ (10 mL). The mixture was stirred at 20 °C for 16 h, then heated to reflux for 2 h, and the solvent was removed under reduced pressure. After the addition of water, extraction with $CH_2Cl_2$, and drying ($Na_2SO_4$), the solvent was evaporated. The crude product was purified by column chromatography (heptane/$CH_2Cl_2$, 20:80) to yield **19a** (116 mg, 36 %). M.p. 88 °C; $^1$H NMR (200.13 MHz, $CDCl_3$): $\delta$ = 7.87 and 7.65 (AA′XX′, $J$(A,X) = 8.5 Hz, 12H), 7.47 and 7.14 (AA′XX′, $J$(A,X) = 8.7 Hz, 12H), 7.23 (d, $J$ = 16.0 Hz, 3H), 7.05 (d, $J$ = 16.0 Hz, 3H), 3.09 (m, 6H), 1.73 (m, 6H), 1.24 (m, 30H), 0.86 ppm (t, $J$ = 6.5 Hz, 9H); $^{13}$C NMR (50.32 MHz, $CDCl_3$): $\delta$ = 147.1, 142.8, 137.1, 132.1, 131.5, 128.5, 128.0, 126.7, 125.4, 124.3, 56.3, 31.6, 28.9, 28.8, 28.2, 22.6, 22.5, 14.0 ppm; HRMS (LSIMS$^+$, mNBA): $m/z$ calcd for $C_{66}H_{81}NO_6S_3$: 1079.5226 $[M^+\cdot]$; found: 1079.5245; elemental analysis calcd (%) for $C_{66}H_{81}NO_6S_3$ (1080.57): C 73.36, H 7.56, N 1.30, S 8.90; found: C 73.08, H 7.49, N 1.15, S 9.08.

*Tris{4-[(1E)-2-(4-{(1E)-2-[4-(octylsulfonyl)phenyl]ethenyl}phenyl)ethenyl]phenyl}amine (**19b**)*

*t*BuOK (70.7 mg, 0.63 mmol) was added to a solution of tris(4-formylphenyl)amine[20] (**18a**) (46.1 mg, 0.14 mmol) and **5** (234 mg, 0.462 mmol) in anhydrous $CH_2Cl_2$ (8 mL). The mixture was stirred at 20 °C for 16 h, then heated to reflux for 4 h, and the solvent was removed under reduced pressure. After the addition of water, extraction with $CH_2Cl_2$, and drying ($Na_2SO_4$), the solvent was evaporated. The crude product was purified by column chromatography (heptane/$CH_2Cl_2$, 40:60) and washed with pentane to yield **19b** (52 mg, 27 %). M.p. 127–129 °C; $^1$H NMR (200.13 MHz, $CDCl_3$): $\delta$ = 7.87 and 7.66 (AA′XX′, $J$(A,X) = 8.4 Hz, 12H), 7.52 (s, 12H), 7.44 and 7.12 (AA′XX′, $J$(A,X) = 8.7 Hz, 12H), 7.25 (d, $J$ = 16.3 Hz, 3H), 7.20 (d, $J$ = 16.0 Hz, 3H), 7.06 (d, $J$ = 16.0 Hz, 3H), 7.02 (d, $J$ = 16.3 Hz, 3H), 3.09 (m, 6H), 1.72 (m, 6H), 1.23 (m, 30H), 0.86 ppm (t, $J$ = 6.3 Hz, 9H); $^{13}$C NMR (50.32 MHz, $CDCl_3$): $\delta$ = 146.7, 142.7, 137.9, 137.3, 135.4, 132.1, 128.5, 127.6, 127.3, 126.9, 126.8, 126.2, 124.3, 56.4, 31.6, 28.93, 28.86, 28.2, 22.7, 22.5, 14.0 ppm; HRMS (ES$^+$, $CH_2Cl_2$/MeOH, 20:80): $m/z$ calcd for $C_{90}H_{99}NO_6NaS_3$: 1408.6532 $[M+Na]^+$; found: 1408.6560.

*Tris{4-[(1E)-2-{4-[(trifluoromethyl)sulfonyl]phenyl}ethenyl]phenyl}amine (**19c**)*

Air was removed from a solution of **18b** (60 mg, 185 μmol) and **3b**[9j] (187 mg, 649 μmol) in anhydrous DMF (1 mL) and $Et_3N$ (0.1 mL, 742 μmol) by blowing argon for 20 min. Then ($o$-tol)$_3$P (17 mg, 55 μmol) and $Pd(OAc)_2$ (7 mg, 28 μmol) were added. The reaction mixture was heated for 3 h at 100 °C. After evaporation of the solvents, the crude product was purified by column chromatography (heptane/$CH_2Cl_2$ 50:50) to yield **19c** (133 mg, 75 %). M.p. 135–136 °C; $^1$H NMR (300.13 MHz, $CDCl_3$): $\delta$ = 8.00 and 7.74 (AA′XX′, $J$(A,X) = 8.5 Hz, 12H), 7.52 and 7.17 (AA′XX′, $J$(A,X) = 8.5 Hz, 12H), 7.33 (d, $J$ = 16.5 Hz, 3H), 7.09 ppm (d, $J$ = 16.5 Hz, 3H); $^{13}$C NMR (75.47 MHz, $CDCl_3$): $\delta$ = 147.5, 145.8, 133.6, 131.2, 128.7, 128.4, 127.1, 127.1, 124.9, 124.5, 119.9 ppm (q, $J$ = 325.9 Hz); $^{19}$F NMR (282.37 MHz, $CDCl_3$): $\delta$ = −78.42 ppm; HRMS (LSIMS$^+$, mNBA): $m/z$ calcd for $C_{45}F_9H_{30}NO_6S_3$: 947.1092 $[M^+\cdot]$; found: 947.1105; elemental analysis calcd (%) for $C_{45}F_9H_{30}NO_6S_3$ (947.93): C 57.02, H 3.19, N 1.48; found: C 56.63, H 3.47, N 1.31.

*Tris{4-[(1E)-2-(4-[(1E)-2-[4-(trifluoromethylsulfonyl)phenyl]ethenyl}phenyl)ethenyl]phenyl}amine (**19d**)*

Air was removed from a solution of **14a** (20.3 mg, 32.6 μmol), **4b** (50.2 mg, 148 μmol), and $K_2CO_3$ (24.5 mg, 177 μmol) in anhydrous DMF (1.5 mL) by blowing argon for 20 min. Then $nBu_4NCl$ (41.1 mg, 148 μmol), $PPh_3$ (2.6 mg, 9.9 μmol), and $Pd(OAc)_2$ (1.1 mg, 4.9 μmol) were added. The reaction mixture was heated at 90 °C for 10 h. After elimination of solvent, the crude product was purified by column chromatography (heptane/$CH_2Cl_2$ 50:50) to yield **19d** (26.5 mg, 65 %). M.p. 199–201 °C; $^1$H NMR (200.13 MHz, $CDCl_3$): $\delta$ = 8.00 and 7.75 (AA′XX′, *J*(A,X) = 8.5 Hz, 12H), 7.55 (s, 12H), 7.45 (d, *J* = 8.7 Hz, 6H), 7.34 (d, *J* = 16.3 Hz, 3H), 7.19–7.11 (m, 12H), 7.03 ppm (d, *J* = 16.3 Hz, 3H); $^{19}$F NMR (282.38 MHz, $CDCl_3$): $\delta$ = −78.44 ppm; HRMS (LSIMS$^+$, mNBA): *m*/*z* calcd for $C_{69}H_{48}F_9NO_6S_3$: 1253.2500 [$M^+$·]; found: 1253.2522; elemental analysis calcd (%) for $C_{69}H_{48}F_9NO_6S_3$ (1254.33): C 66.07, H 3.86, N 1.12, S 7.67; found: C 65.92, H 3.98, N 1.22, S 7.54.

*Tris{4-[(1E)-2-{4-[(nonafluorobutyl)sulfonyl]phenyl}ethenyl]phenyl}amine (**19e**)*

The reaction of **18b** (41.7 mg, 0.129 mmol) with **11** (226.5 mg, 0.516 mmol) was as described for **19c**, with subsequent purification by column chromatography (heptane/$CH_2Cl_2$ 60:40), to afford **19e** (100 mg, 55 %). M.p. 137–138 °C; $^1$H NMR (200.13 MHz, $CDCl_3$): $\delta$ = 7.99 and 7.74 (AA′XX′, *J*(A,X) = 8.2 Hz, 12H), 7.51 and 7.17 (AA′XX′, *J*(A,X) = 8.6 Hz, 12H), 7.32 (d, *J* = 16.2 Hz, 3H), 7.08 ppm (d, *J* = 16.2 Hz, 3H); $^{19}$F NMR (282.37 MHz, $CDCl_3$): $\delta$ = −80.63 (m, 9F), −110.66 (t, *J* = 13.8 Hz, 6F), −120.79 (m, 6F), −125.8985 ppm (m, 6F); HRMS (ES$^+$, MeOH/$CH_2Cl_2$, 95:5): *m*/*z* calcd for $C_{54}H_{30}NO_6F_{27}KS_3$: 1436.0441 [*M*+K]$^+$; found: 1436.0479.

*Tris{4-[(1E)-2-{9,9-dinonyl-7-[(1E)-2-{4-[(trifluoromethyl)sulfonyl]phenyl}ethenyl]-9H-fluoren-2-yl}ethenyl]phenyl}amine (**20**)*

*t*BuOK (120 mg, 1.07 mmol) was added to a solution of **8b** (450 mg, 0.786 mmol) and **1b** (257 mg, 0.714 mmol) in anhydrous $CH_2Cl_2$ (30 mL). The reaction mixture was stirred for 15 h in the dark. After evaporation of the solvent, the residue was purified by column chromatography (heptane/$CH_2Cl_2$ 60:40) to yield **9** (102 mg, 18 %; as a mixture of *E*/*Z* stereoisomers). The reaction of **18b** (10 mg, 31 μmol) with **9** (97 mg, 124 μmol) was as described for **19c**, for 15 h at 110 °C, with subsequent purification by column chromatography (heptane/$CH_2Cl_2$, gradient from 70:30 to 50:50) to afford **20** (12 mg, 18 %). $^1$H NMR (500.13 MHz, $CDCl_3$): $\delta$ = 7.99 and 7.77 (AA′XX′, *J*(A,X) = 8.4 Hz, 12H), 7.69 (d, *J* = 8.2 Hz, 3H), 7.67 (d, *J* = 8.2 Hz, 3H), 7.54 (d, *J* = 8.2 Hz, 3H), 7.52 (d, *J* = 8.2 Hz, 3H), 7.49 and 7.14 (AA′XX′, *J*(A,X) = 8.4 Hz, 12H), 7.49–7.42 (m, 12H), 7.42 (d, *J* = 16.3 Hz, 3H), 7.19 (d, *J* = 16.3 Hz, 3H), 2.01 (m, 12H), 1.23–1.05 (m, 72H), 0.79 (t, *J* = 7 Hz, 18H), 0.66 ppm (m, 12H); $^{19}$F NMR (282.37 MHz, $CDCl_3$): $\delta$ = −78.40 ppm; HRMS (ES$^+$, MeOH): *m*/*z* calcd for $C_{144}H_{168}NO_6S_3F_9K$: 2313.15272 [*M*+K]$^+$; found: 2313.1865.

*Spectroscopic Measurements*

All photophysical properties were performed with freshly prepared air-equilibrated solutions at room temperature (298 K). UV/Vis absorption spectra were recorded with a Jasco V-570 spectrophotometer. Steady-state and time-resolved fluorescence measurements were performed on dilute solutions (ca. $10^{-6}$ M, optical density < 0.1) contained in standard 1 cm quartz cuvettes with an Edinburgh Instruments (FLS920) spectrometer in photon-counting mode. Fully corrected emission spectra were obtained for each compound under excitation at the wavelength of the absorption maximum, with $A_{\lambda ex} < 0.1$ to minimize internal absorption. Fluorescence quantum yields were measured according to literature procedures using fluorescein in 0.1 M NaOH as a standard (quantum yield $\Phi$ = 0.90).[33] Fluorescence lifetimes were measured by time-correlated single-photon counting (TCSPC). Excitation was achieved by a hydrogen-filled nanosecond flashlamp (repetition rate 40 kHz). The instrument response (FWHM ca. 1 ns) was determined by measuring the light scattered by a Ludox suspension. The TCSPC traces were analyzed by standard iterative reconvolution methods implemented in the software of the fluorimeter. All compounds displayed strictly monoexponential fluorescence decays ($\chi^2 < 1.1$). The reported lifetimes are within ±0.1 ns.

*Two-Photon Absorption Experiments*

To span the 700–980 nm range, a Nd:YLF-pumped Ti:sapphire oscillator was used to generate 150 fs pulses at a 76 MHz rate. The excitation was focused into the cuvette through a microscope objective (10×/NA 0.25). The applied average laser power that arrived at the sample was between 0.5 and 15 mW, thereby leading to a time-averaged light flux in the focal volume on the order of 0.1–1 mW μm$^{-2}$. The generated fluorescence was collected in epifluorescence mode, through the microscope objective, and reflected by a dichroic mirror (675dcxru, Chroma Technology Corporation, USA). This makes it possible to avoid the inner filter effects related to the high dye concentrations used ($10^{-4}$ M) by focusing the laser near the cuvette window. Residual excitation light was removed using a barrier filter (e650-2p, Chroma), and the fluorescence was coupled into a 600 μm multimode fiber by an achromatic doublet. The fiber was connected to a compact CCD-based spectrometer (BTC112-E, B&WTek, USA), which measured the two-photon excited emission spectrum. Total fluorescence intensities were obtained by integrating the corrected emission spectra measured by this spectrometer. 2PA cross-sections ($\sigma_2$) were determined from the two-photon excited fluorescence (2PEF) cross-sections ($\sigma_2\Phi$) and the fluorescence emission quantum yield ($\Phi$). 2PEF cross-sections of $10^{-4}$ M toluene solutions were measured relative to fluorescein in 0.01 M aqueous NaOH for 715–980 nm[9b,28] by using the well-established method described by Xu and Webb[28] and the appropriate solvent-related refractive index corrections.[34] The experimental uncertainty on the absolute action cross-sections determined by this method has been estimated to be ±20 %.[28] The quadratic dependence of the fluorescence intensity on the excitation power was checked for each sample and all wavelengths (see examples of quadratic dependences in the Supporting Information), thus indicating that the measurements were carried out in intensity regimes in which saturation or photodegradation did not occur.

*Cell Imaging Methods*

HEK293 was routinely cultured in Dulbecco's modified eagle's medium (DMEM) supplemented with 10 % fetal calf serum (FCS), D-glucose, sodium pyruvate, penicillin/streptomycin, and nonessential amino acids, and maintained in a humid incubator at 37 °C in 5 % $CO_2$, in a 75 cm$^2$ tissue culture flask. For confocal analysis, HEK cells were grown on phenol-red-free DMEM supplemented with 10 % FCS without steroid (FCS-DCC) in a cover slip in a six-well culture plate. Cells were split at a ratio of 1/2 or 1/3 every 3 days. One day after the split, a solution (6 μL) of 1 mM fluorophores was added into phenol-red-free DMEM (2 mL) for 2 h incubation. The well was washed with PBS, then fresh phenol-red-free DMEM (2 mL) supplemented with FCS-DCC was added and incubated for 24 h. The old media was removed and the cover slip was analyzed with a confocal microscope.

## Acknowledgements

Région Bretagne is acknowledged for a fellowship to C.L.D and A.S. (DEMASIDA and BIPHOBIO grants). M.B.D. gratefully thanks the Conseil Régional d'Aquitaine for generous funding (Chaire d'Accueil grant). We gratefully thank Charlotte Brigand and Frédéric Percevault (IRSET INSERM U 1085, University of Rennes 1) for cell culture and staining, and Emmanuel Schaub from the PIXEL platform (multiphoton microscopy facilities, University of Rennes 1) for expert assistance in bio-imaging experiments.

[1] a) G. S. He, L.-S. Tan, Q. Zheng, P. N. Prasad, *Chem. Rev.* **2008**, *108*, 1245–1330; b) F. Terenziani, C. Katan, E. Badaeva, S. Tretiak, M. Blanchard-Desce, *Adv. Mater.* **2008**, *20*, 4641–4678; c) H. M. Kim, B. R. Cho, *Chem. Commun.* **2009**, 153–164; d) M. Pawlicki, H. A.

Collins, R. G. Denning, H. L. Anderson, *Angew. Chem.* **2009**, *121*, 3292–3316; *Angew. Chem. Int. Ed.* **2009**, *48*, 3244–3266.

[2] a) W. Denk, J. H. Strickler, W. W. Webb, *Science* **1990**, *248*, 73–76; b) C. Xu, W. Zipfel, J. B. Shear, R. M. Williams, W. W. Webb, *Proc. Natl. Acad. Sci. USA* **1996**, *93*, 10763–10768; c) H. M. Kim, B. R. Cho, *Acc. Chem. Res.* **2009**, *42*, 863–872; d) S. Yao, K. D. Belfield, *Eur. J. Org. Chem.* **2012**, 3199–3217.

[3] a) J. D. Bhawalkar, N. D. Kumar, C. F. Zhao, P. N. Prasad, *J. Clin. Laser Med. Surg.* **1997**, *15*, 201–204; b) S. Kim, T. Y. Ohulchanskyy, H. E. Pudavar, R. K. Pandey, P. N. Prasad, *J. Am. Chem. Soc.* **2007**, *129*, 2669–2675; c) H. A. Collins, M. Khurana, E. H. Moriyama, A. Mariampillai, E. Dahlstedt, M. Balaz, M. K. Kuimova, M. Drobizhev, V. X. D. Yang, D. Phillips, A. Rebane, B. C. Wilson, H. L. Anderson, *Nat. Photonics* **2008**, *2*, 420–424; d) J. R. Starkey, A. K. Rebane, M. A. Drobizhev, F. Meng, A. Gong, A. Elliott, K. McInnerney, C. W. Spangler, *Clin. Cancer Res.* **2008**, *14*, 6564–6573; e) B. W. Pedersen, T. Breitenbach, R. W. Redmond, P. R. Ogilby, *Free Radical Res.* **2010**, *44*, 1383–1397; f) M. Gary-Bobo, Y. Mir, C. Rouxel, D. Brevet, I. Basile, M. Maynadier, O. Vaillant, O. Mongin, M. Blanchard-Desce, A. Morère, M. Garcia, J.-O. Durand, L. Raehm, *Angew. Chem.* **2011**, *123*, 11627–11631; *Angew. Chem. Int. Ed.* **2011**, *50*, 11425–11429; g) X. Yue, C. O. Yanez, S. Yao, K. D. Belfield, *J. Am. Chem. Soc.* **2013**, *135*, 2112–2115.

[4] a) T. Furuta, S. S. H. Wang, J. L. Dantzker, T. M. Dore, W. J. Bybee, E. M. Callaway, W. Denk, R. Y. Tsien, *Proc. Natl. Acad. Sci. USA* **1999**, *96*, 1193–1200; b) G. C. R. Ellis-Davies, M. Matsuzaki, M. Paukert, H. Kasai, D. E. Bergles, *J. Neurosci.* **2007**, *27*, 6601–6604; c) M. Matsuzaki, T. Hayama, H. Kasai, G. C. R. Ellis-Davies, *Nat. Chem. Biol.* **2010**, *6*, 255–257; d) G. C. R. Ellis-Davies, *ACS Chem. Neurosci.* **2011**, *2*, 185–197.

[5] a) D. A. Parthenopoulos, P. M. Rentzepis, *Science* **1989**, *245*, 843–845; b) J. H. Strickler, W. W. Webb, *Opt. Lett.* **1991**, *16*, 1780–1782.

[6] a) G. S. He, G. C. Xu, P. N. Prasad, B. A. Reinhardt, J. C. Bhatt, R. McKellar, A. G. Dillard, *Opt. Lett.* **1995**, *20*, 435–437; b) J. E. Ehrlich, X. L. Wu, I. Y. S. Lee, Z. Y. Hu, H. Röckel, S. R. Marder, J. W. Perry, *Opt. Lett.* **1997**, *22*, 1843–1845.

[7] a) S. Maruo, O. Nakamura, S. Kawata, *Opt. Lett.* **1997**, *22*, 132–134; b) B. H. Cumpston, S. P. Ananthavel, S. Barlow, D. L. Dyer, J. E. Ehrlich, L. L. Erskine, A. A. Heikal, S. M. Kuebler, I.-Y. S. Lee, D. McCord-Maughon, J. Qin, H. Röckel, M. Rumi, X. L. Wu, S. R. Marder, J. W. Perry, *Nature* **1999**, *398*, 51–54; c) S. Kawata, H.-B. Sun, T. Tanaka, K. Takada, *Nature* **2001**, *412*, 697–698; d) W. Zhou, S. M. Kuebler, K. L. Braun, T. Yu, J. K. Cammack, C. K. Ober, J. W. Perry, S. R. Marder, *Science* **2002**, *296*, 1106–1109; e) F. Claeyssens, E. A. Hasan, A. Gaidukeviciute, D. S. Achilleos, A. Ranella, C. Reinhardt, A. Ovsianikov, X. Shizhou, C. Fotakis, M. Vamvakaki, B. N. Chichkov, M. Farsari, *Langmuir* **2009**, *25*, 3219–3223; f) M. Farsari, M. Vamvakaki, B. N. Chichkov, *J. Opt.* **2010**, *12*, 124001–124016.

[8] a) L. Ventelon, S. Charier, L. Moreaux, J. Mertz, M. Blanchard-Desce, *Angew. Chem.* **2001**, *113*, 2156–2159; *Angew. Chem. Int. Ed.* **2001**, *40*, 2098–2101; b) M. Blanchard-Desce, *C. R. Phys.* **2002**, *3*, 439–448; c) M. H. V. Werts, S. Gmouh, O. Mongin, T. Pons, M. Blanchard-Desce, *J. Am. Chem. Soc.* **2004**, *126*, 16294–16295; d) C. Le Droumaguet, O. Mongin, M. H. V. Werts, M. Blanchard-Desce, *Chem. Commun.* **2005**, 2802–2804; e) T. R. Krishna, M. Parent, M. H. V. Werts, L. Moreaux, S. Gmouh, S. Charpak, A.-M. Caminade, J.-P. Majoral, M. Blanchard-Desce, *Angew. Chem.* **2006**, *118*, 4761–4764; *Angew. Chem. Int. Ed.* **2006**, *45*, 4645–4648; f) M.-H. Ha-Thi, M. Penhoat, D. Drouin, M. Blanchard-Desce, V. Michelet, I. Leray, *Chem. Eur. J.* **2008**, *14*, 5941–5950.

[9] a) B. A. Reinhardt, L. L. Brott, S. J. Clarson, A. G. Dillard, J. C. Bhatt, R. Kannan, L. Yuan, G. S. He, P. N. Prasad, *Chem. Mater.* **1998**, *10*, 1863–1874; b) M. A. Albota, C. Xu, W. W. Webb, *Appl. Opt.* **1998**, *37*, 7352–7356; c) L. Ventelon, L. Moreaux, J. Mertz, M. Blanchard-Desce, *Chem. Commun.* **1999**, 2055–2056; d) P. K. Frederiksen, M. Jørgensen, P. R. Ogilby, *J. Am. Chem. Soc.* **2001**, *123*, 1215–1221; e) O. Mongin, L. Porrès, L. Moreaux, J. Mertz, M. Blanchard-Desce, *Org. Lett.* **2002**, *4*, 719–722; f) A. Abbotto, L. Beverina, R. Bozio, A. Facchetti, C. Ferrante, G. A. Pagani, D. Pedron, R. Signorini, *Org. Lett.* **2002**, *4*, 1495–1498; g) W. J. Yang, D. Y. Kim, M.-Y. Jeong, H. M. Kim, S.-J. Jeon, B. R. Cho, *Chem. Commun.* **2003**, 2618–2619; h) S. K. Lee, W. J. Yang, J. J. Choi, C. H. Kim, S.-J. Jeon, B. R. Cho, *Org. Lett.* **2005**, *7*, 323–326; i) C. B. Nielsen, M. Johnsen, J. Arnbjerg, M. Pittelkow, S. P. McIlroy, P. R. Ogilby, M. Jorgensen, *J. Org. Chem.* **2005**, *70*, 7065–7079; j) O. Mongin, L. Porrès, M. Charlot, C. Katan, M. Blanchard-Desce, *Chem. Eur. J.* **2007**, *13*, 1481–1498; k) S. Yao, H.-Y. Ahn, X. Wang, J. Fu, E. W. Van Stryland, D. J. Hagan, K. D. Belfield, *J. Org. Chem.* **2010**, *75*, 3965–3974; l) C. D. Andrade, C. O. Yanez, L. Rodriguez, K. D. Belfield, *J. Org. Chem.* **2010**, *75*, 3975–3982; m) H.-Y. Ahn, S. Yao, X. Wang, K. D. Belfield, *ACS Appl. Mater. Interfaces* **2012**, *4*, 2847–2854.

[10] a) S.-J. Chung, K.-S. Kim, T.-C. Lin, G. S. He, J. Swiatkiewicz, P. N. Prasad, *J. Phys. Chem. B* **1999**, *103*, 10741–10745; b) L. Porrès, O. Mongin, C. Katan, M. Charlot, T. Pons, J. Mertz, M. Blanchard-Desce, *Org. Lett.* **2004**, *6*, 47–50; c) C. Rouxel, C. Le Droumaguet, Y. Macé, S. Clift, O. Mongin, E. Magnier, M. Blanchard-Desce, *Chem. Eur. J.* **2012**, *18*, 12487–12497; d) P. Hrobárik, V. Hrobáriková, I. Sigmundová, P. Zahradník, M. Fakis, I. Polyzos, P. Persephonis, *J. Org. Chem.* **2011**, *76*, 8726–8736.

[11] a) B. R. Cho, K. H. Son, S. H. Lee, Y.-S. Song, Y.-K. Lee, S.-J. Jeon, J. H. Choi, H. Lee, M. Cho, *J. Am. Chem. Soc.* **2001**, *123*, 10039–10045; b) Y.-Z. Cui, Q. Fang, G. Xue, G.-B. Xu, L. Yin, W.-T. Yu, *Chem. Lett.* **2005**, *34*, 644–645; c) G. Argouarch, R. Veillard, T. Roisnel, A. Amar, H. Meghezzi, A. Boucekkine, V. Hugues, O. Mongin, M. Blanchard-Desce, F. Paul, *Chem. Eur. J.* **2012**, *18*, 11811–11827; d) Y. M. Poronik, V. Hugues, M. Blanchard-Desce, D. T. Gryko, *Chem. Eur. J.* **2012**, *18*, 9258–9266.

[12] C. Katan, F. Terenziani, O. Mongin, M. H. V. Werts, L. Porrès, T. Pons, J. Mertz, S. Tretiak, M. Blanchard-Desce, *J. Phys. Chem. A* **2005**, *109*, 3024–3037.

[13] V. Alain-Rizzo, D. Drouin-Kucma, C. Rouxel, I. Samb, J. Bell, P. Y. Toullec, V. Michelet, I. Leray, M. Blanchard-Desce, *Chem. Asian J.* **2011**, *6*, 1080–1091.

[14] F. Terenziani, C. Le Droumaguet, C. Katan, O. Mongin, M. Blanchard-Desce, *ChemPhysChem* **2007**, *8*, 723–734.

[15] C. Hansch, A. Leo, R. W. Taft, *Chem. Rev.* **1991**, *91*, 165–195.

[16] Y. Le Bigot, M. Delmas, A. Gaset, *Synth. Commun.* **1983**, *13*, 177–182.

[17] M. Jessing, M. Brandt, K. J. Jensen, J. B. Christensen, U. Boas, *J. Org. Chem.* **2006**, *71*, 6734–6741.

[18] C. G. J. Verhart, G. I. Tesser, *Recl. Trav. Chim. Pays-Bas* **1988**, *107*, 621–626.

[19] Y. Shirota, T. Kobata, N. Noma, *Chem. Lett.* **1989**, 1145–1148.

[20] T. Mallegol, S. Gmouh, M. A. A. Meziane, M. Blanchard-Desce, O. Mongin, *Synthesis* **2005**, 1771–1774.

[21] T. Jeffery, *Tetrahedron* **1996**, *52*, 10113–10130.

[22] Fluorescence quantum yields determined relative to quinine bisulfate in 0.5 M $H_2SO_4$ are in good agreement with those determined relative to fluorescein in 0.1 M NaOH.

[23] S. J. Strickler, R. A. Berg, *J. Chem. Phys.* **1962**, *37*, 814–822.

[24] a) E. Lippert, *Z. Naturforsch. A* **1955**, *10*, 541–545; b) N. Mataga, Y. Kaifu, M. Koizumi, *Bull. Chem. Soc. Jpn.* **1955**, *28*, 690–691.

[25] We also checked that viscosity was not influencing the position of the fluorescence band but rather the fluorescence quantum yield (increased viscosity would lead to larger fluorescence quantum yield).

[26] G. F. Mes, B. de Jong, H. J. van Ramesdonk, J. W. Verhoeven, J. M. Warman, M. P. de Haas, L. E. W. Horsman-van den Dool, *J. Am. Chem. Soc.* **1984**, *106*, 6524–6528.

[27] C. Katan, M. Charlot, O. Mongin, C. L. Le Droumaguet, V. Jouikov, F. Terenziani, E. Badaeva, S. Tretiak, M. Blanchard-Desce, *J. Phys. Chem. B* **2010**, *114*, 3152–3169.

[28] C. Xu, W. W. Webb, *J. Opt. Soc. Am. B* **1996**, *13*, 481–491.

[29] A. Ulman, C. S. Willand, W. Köhler, D. R. Robello, D. J. Williams, L. Handley, *J. Am. Chem. Soc.* **1990**, *112*, 7083–7090.

[30] M. S. Wong, M. Samoc, A. Samoc, B. Luther-Davies, M. G. Humphrey, *J. Mater. Chem.* **1998**, *8*, 2005–2009.

[31] S. Rozen, Y. Bareket, *J. Org. Chem.* **1997**, *62*, 1457–1462.
[32] F. Würthner, H.-W. Schmidt, F. Haubner, *Ger. Offen.* **1998**, DE 96–19643097.
[33] a) J. N. Demas, G. A. Crosby, *J. Phys. Chem.* **1971**, *75*, 991–1024; b) D. F. Eaton, *Pure Appl. Chem.* **1988**, *60*, 1107–1114.
[34] M. H. V. Werts, N. Nerambourg, D. Pélégry, Y. Le Grand, M. Blanchard-Desce, *Photochem. Photobiol. Sci.* **2005**, *4*, 531–538.

Received: May 30, 2013
Revised: July 3, 2013
Published online: ■■ ▮▮, 0000

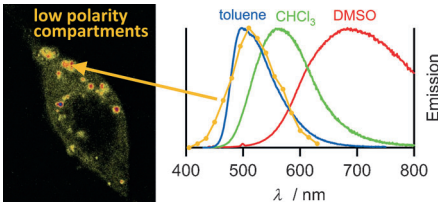


**Core values**: A series of octupolar fluorophores built from a triphenylamine core connected to electron-withdrawing peripheral groups through conjugated spacers has been synthesized. Their photoluminescence, solvatochromism, and two-photon absorption properties were systematically investigated to derive structure–property relationships.

**Bioimaging**

*Céline Le Droumaguet, Aude Sourdon, Emilie Genin, Olivier Mongin,* Mireille Blanchard-Desce** _ ▮▮▮▮–▮▮▮▮

**Two-Photon Polarity Probes Built from Octupolar Fluorophores: Synthesis, Structure–Properties Relationships, and Use in Cellular Imaging**